Deltares

Gel barriers in the Port of Rotterdam

Analysis of the hydrodynamics, sediment transport and stability

Fi

Gel barriers in the Port of Rotterdam
Analysis of the hydrodynamics, sediment transport and stability

Author(s)
Lynyrd de Wit
Luka Jaksic

Gel barriers in the Port of Rotterdam
Analysis of the hydrodynamics, sediment transport and stability

Opdrachtgever	TKI consortium of Port of Rotterdam (PoR), Rijkswaterstaat (RWS), TU Delft, Royal HaskoningDHV, SmartPort and Deltares.
Contactpersoon	TKI consortium
Referenties	Referenties
Trefwoorden	Maintenance dredging innovation, flocculant, gel barrier, fluid mud, port sedimentation, Port of Rotterdam

Documentgegevens	
Versie	1.0
Datum	15-11-2022
Projectnummer	11207279-000
Document ID	11207279-000-ZKS-0001
Pagina's	52
Classificatie	
Status	final

Auteur(s)		
	Lynyrd de Wit	
	Luka Jaksic	

Onderstaande tabel is niet voor publicatie

Doc. Versie	**Auteur**	**Controle**	**Akkoord**
1.0	Lynyrd de Wit	Thijs van Kessel	Toon Segeren
	Luka Jaksic		

Summary

This report describes the results of Phase 2 of the TKI feasibility study on the application of gel barriers in ports to control sediment transport and sedimentation. The TKI consortium consists of Port of Rotterdam (PoR), Rijkswaterstaat (RWS), TU Delft, Royal HaskoningDHV, SmartPort and Deltares. In Phase 1 of this research, a stable gel that can be used for making gel barriers was designed by a PDEng student of the TU Delft (Bampatzeliou, et al., 2022). Phase 2 focusses on the ability of a gel barrier to reduce sedimentation and its interaction with navigation and flow conditions in the Port of Rotterdam.

Dredging efforts in the Port of Rotterdam are associated with high yearly costs and emissions. Gel barriers are biodegradable obstacles which could be placed on the bottom of a port entrance to reduce the spreading of sediments into certain port areas, and thus save on dredging expenses and emissions. Ideally, gel barriers should not obstruct navigation for vessels. Gel barriers are a combination of dredged material (i.e., excess sediment) and a biological flocculating agent, which should result in a stable yet eco-friendly barrier.

Based on lab experiments and numerical simulations, it can be concluded that the inland harbors of the PoR – such as Botlek – are most suitable to construct a barrier in terms of gel stability and the gel barrier's potential to reduce sedimentation. In inland harbors the flow conditions are generally mild, so that a gel barrier can withstand the natural flow currents and the water column is stratified which enhances its ability in steering sedimentation.

Lab experiments are used to approximate the gels' erosion thresholds. A 100 Pa BYS (Bingham Yield Stress) gel, which is expected to be navigable, does not erode for near-bottom velocities below 0.6 m/s. This gel is most suitable to construct a barrier in the more sheltered areas in the port like the entrances of Botlek/3e Petroleumhaven, Waalhaven and the Calandkanaal, where the tidal and river flow induced bed shear stresses remain below the gel's erosion threshold. For the parts of the port with stronger currents, the stiffer 400 Pa BYS gel might remain stable as its erosion threshold is expected to be > 1 m/s. It is however the question whether such a stiff gel is navigable.

Apart from the ambient conditions also propeller jets of passing vessels affect the gel's stability. The propeller jet impact on a gel barrier is investigated by using CFD simulations. The propeller jet of a representative large vessel that is expected to sail into Botlek several times per week is found to inflict velocities on the gel barrier which are higher than the 100 Pa gel's erosion threshold when the gap between keel and gel barrier is below 2 m. In those situations, damage to the gel barrier is expected to occur. It requires further research to investigate how effective a gel barrier is after a large vessel has passed with its keel close to the gel barrier and how a gel barrier could be maintained after such event.

The results of a large-scale sediment transport model suggest that the barrier is most effective in reducing sedimentation in the inland harbors with little vertical mixing and thus a concentrated near-bed layer of suspended sediment. Of the investigated locations, the barrier was found to be most effective in the Botlek/3Pet basin, where the sedimentation rate is reduced with roughly 17% for a 3 m-high barrier. Most of this sediment mass (80%) settles within 15 km from the Botlek in the main waterways/rivers, 15% of which can be found landward leading to extra sailing distance for the dredger and 65% seaward leading to a reduction in sailing distance. Although this study does not quantify the potential saving in terms of costs or CO_2 emissions, these results suggest that a barrier could benefit dredging operations.

All in all, the gel barrier has a very interesting combination of features. It can limit and steer sedimentation and as a material it has some strength while being flexible at the same time. The gel barrier has the potential to reduce dredging efforts (and, hence, costs and emissions), by reducing sailing distances and reducing dredging operations in less accessible and potentially contaminated basins. This applies especially to the inland harbors, such as the Botlek. Gel barriers are especially effective in stratified systems and the effectiveness increases with a barrier height of more than 2m.

The most important remaining knowledge gaps are the costs of the gel barriers vs its benefits, as well as the stability of the barrier in time under different failure mechanisms, and the question of gel barrier effectiveness and required maintenance after ship propeller damage. Recommendations are provided on how to fill in those knowledge gaps.

Table of content

1 Introduction

This report describes the results of Phase 2 of the TKI feasibility study on the application of gel barriers in ports to control sediment transport and sedimentation. In Phase 1 of this research, a stable gel that can be used for making gel barriers was designed by a PDEng student of the TU Delft (Bampatzeliou, et al., 2022). Phase 2 focusses on the ability of a gel barrier to reduce sedimentation and its interaction with navigation and flow conditions in the Port of Rotterdam.

1.1 Context

Every year, roughly 15-20 million cubic meters of sediment are dredged in the Port of Rotterdam to keep the port navigable. This effort is associated with high annual costs and emissions. Furthermore, the presence of contaminated sediments in ports may enhance the complexity of these dredging operations. In a TKI consortium with the Port of Rotterdam (PoR), Rijkswaterstaat (RWS), TU Delft, Royal HaskoningDHV and SmartPort, Deltares is studying whether gel barriers can be used to tackle these challenges.

Gel barriers are biodegradable obstacles which could be placed on the bottom of a port entrance to reduce the spreading of sediments into certain port areas (Figure 1-1). Gel barriers are a combination of dredged material (i.e., excess sediment) and a biological flocculating agent, which should result in a stable yet eco-friendly barrier.

In particular for inland harbors, where dredging is associated with long sailing distances to the offshore disposal sites, gel barriers might be useful to lower dredging costs and emissions. This is especially true if sediment that would otherwise settle in a harbor basin settles closer to the river mouth (and thus the offshore disposal site). A gel barrier could also be used to keep contaminated sediments from spreading into specific port areas if they are concentrated near the bottom (see right panel Figure 1.1).

A gel barrier should be sufficiently stable to endure the flow conditions in the Port of Rotterdam, while it should not obstruct navigation for vessels. A barrier should be sufficiently durable and/or cheap such that the dredging savings outweigh its material, production, placement and maintenance costs and/or emissions.

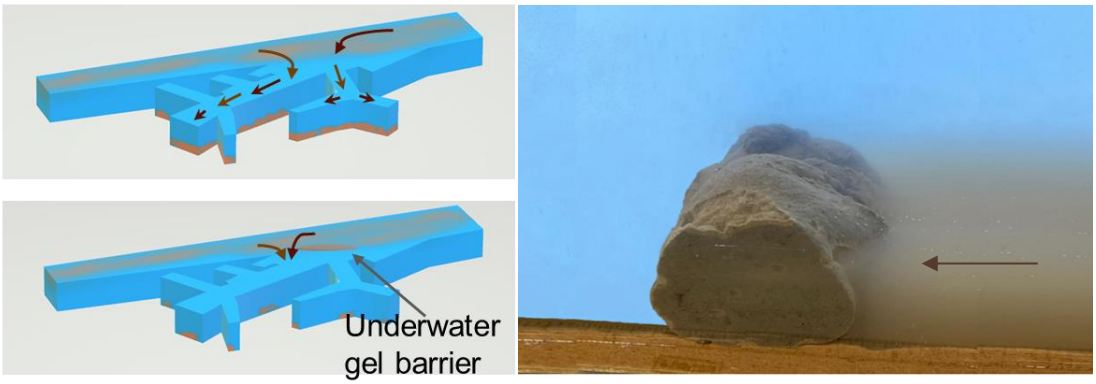

Figure 1-1 Intended operation of a gel barrier. Left: sediment intrusion in the Botlek and 3rd Petroleum harbor without (top) and with a gel barrier (bottom). Right: small scale experiment which illustrates how a gel barrier, constructed with Calandkanaal mud and Xanthan gum, could stop a sediment density currents. Figures are from Bampatzeliou et al. (2022).

1.2 Reader's guide

In Chapter 2, we describe the methods that are used to study the stability of a gel barrier and its effectiveness in reducing sedimentation in the Port of Rotterdam.

The stability of the gel is assessed in Chapter 3. This is done to improve our understanding of what flow conditions the gel could endure.

Next, we study what flow conditions typically occur in the different basins of the PoR to gain insight in the most promising locations to construct a gel barrier in terms of stability or longevity (Chapter 4).

Finally, we select three harbor basins which are most suited for the construction of a gel barrier in terms of flow exposure. For these basins, we study the barrier's potential to reduce sedimentation and thus dredging costs (Chapter 5).

Conclusions and recommendations for further research are presented in Chapter 6.

2 Method

This chapter describes the methods that are used to assess the gel's strength (requirements) and its potential to reduce sedimentation in the PoR.

2.1 Approach

First, lab experiments with varied flow conditions are carried out to study what flow conditions the gel could withstand (see Chapter 3 - Gel stability). The micro-stability of the gel is investigated both qualitatively (with images) and quantitatively (by approximating the erosion threshold). The gel recipes and lab experiments that are used to achieve this are described in Sections 2.2 and 2.3, respectively. It should be noted that this study does not examine the gel barrier's macro-stability (e.g., failure by tumbling or translating of the barrier).

Next, we study if the approximated erosion threshold is exceeded by the flow conditions that typically occur throughout the PoR (see Chapter 4 – Gel stability for PoR flow conditions). A large-scale hydrodynamic model is used to study the exceedance probability of the approximated erosion threshold at various locations throughout the PoR. The used model (setup) is described in Section 2.4.1. In addition, CFD simulations are used to get a first indication on the exposure and damage realized by the propeller of a vessel. The CFD model is described in Section 2.5.

Finally, we select three harbor basins which are most suited for the construction of a gel barrier in terms of flow exposure. For these basins, we study the barrier's potential to reduce sedimentation and thus dredging costs (Chapter 5 – Potential sedimentation reduction by gel barriers). This is done by implementing the barriers in the large-scale numerical model, the setup of which is described in Section 2.4.2.

Figure 2-1 summarizes the methods used in this study.

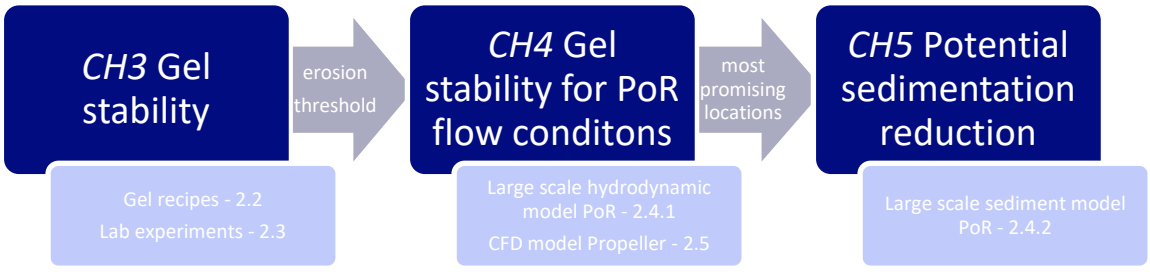

Figure 2-1 Chapters in this report (dark blue) and sections in this chapter where the corresponding methods are described (light blue). Arrows indicate the key result per chapter.

2.2 Gel recipes

In this study, we test the stability of three gel recipes with a Bingham Yield Strength (BYS) of 100, 200 and 400 Pa, respectively (Table 2-1). Their bulk density varies between 1070 and 1210 kg/m^3.

In the first phase of this study, Bampatzeliou et al. (2022) found that Xanthan Gum (right panel), a polysaccharide polymer, has promising properties for the application of a gel barrier in terms production costs/effort, stability and durability.

Xanthan Gum (XG) is readily used on large scale in the food industry and even in dyke projects as a stabilization agent for soil. By mixing local mud from the port with small quantities of XG (0-3% mass) a wide range of Bingham Yield Strengths can be realized (0-400 Pa) by varying the solids and/or XG content.

The mud used for the gels originates from the Calandkanaal and is mixed with 1.6% NaCl w/w water. A hand mixer is used to combine the Xanthan gum (XG) with mud and create a homogenous gel material. A variation in Bingham Yield Strength (BYS) and bulk density is realized by varying both the Xanthan Gum and mud content. The BYS is measured with the parallel plate method using a Haake Mars Rheometer. The bulk density is approximated with a syringe by performing 12 repetitions.

A mass fraction of 3% XG and 20% mud results in a gel with a BYS of 400 Pa and a bulk density of roughly 1200 kg/m^3 (XG3Mud20 in Table 2-1). A mass fraction of 1% and 10% XG mud results in a BYS of 100 Pa and bulk density of roughly 1100 kg/m^3 (XG1Mud10_v2 in Table 2-1). An intermediate strength of 200 Pa was accidently realized and is also used in this study (XG1Mud10_v1 in Table 2-1). From now on the gels are referred to by their BYS.

Table 2-1 Rheological properties of the gel recipes tested in this study. The name contains the mass fraction of Xanthan Gum and mud, respectively. For example, XG3Mud20 means 3% Xanthan Gum and 20% dry mud. The remaining mass fraction is water (NaCl + H_2O).

Name	Bingham Yield Strength (BYS) [Pa]	Bulk density [kg/m^3]
XG3Mud20	400	+/- 1200
XG1Mud10_v1	200	+/- 1100
XG1Mud10_v2	100	+/- 1100

The 100 Pa gel represents a gel that would not obstruct navigation if a vessel would sail into the barrier. Based on experiments in several ports around the world, it was found that fluid mud layers with densities up to 1200 kg/m^3 remain navigable. Furthermore, the German port of Emden prescribes that fluid mud is navigable up till 100 Pa (Kirichek, et al., 2018). XG1Mud10_v2 has properties within these limits (Table 2-1). The 400 Pa gel (XG3Mud20) represents a material that could be used in locations where more strength is required, and where the draught of vessels is not limited.

Bampatzeliou et al., (2022) showed that the gel's strength is time-dependent. Therefore, all lab experiments have been conducted in the first week of the gels' lifetime. The time development of the gel's strenght behaviour remains outside the scope of this study.

For a complete overview of the gel's characteristics, we refer to Bampatzeliou et al. (2022).

2.3 Lab experiments to assess gel stability

Two lab devices that expose the gel to a flow-induced shear stress, are used to study the gels' (micro) stability and measure its erosion threshold.

2.3.1 Gust chamber

The first measurement device is a gust chamber, which has a calibrated shear stress range between 0 and 0.65 Pa. A gust chamber is widely used to measure the erodibility of fine-grained sediments. The device uses a combination of a spinning disk and a central suction to generate a nearly uniform shear stress across a surface in a cylindrical container (Figure 2-2).

The spinning disk on top of the water column initiates a rotational flow that is associated with centrifugal forces. The disk pumps water (and potentially eroded sediment) away from the middle of the water column to compensate for the central fugal forces and to enable a more uniform bed shear stress. The same discharge is moreover pumped into the system to compensate for the outflow. The rotation speed of the disk and the pump discharge are calibrated to enable an accurate bed shear stress at the gel-water interface according to method by Gust (US Patent No. 4884892 A and No. 4973165 A).

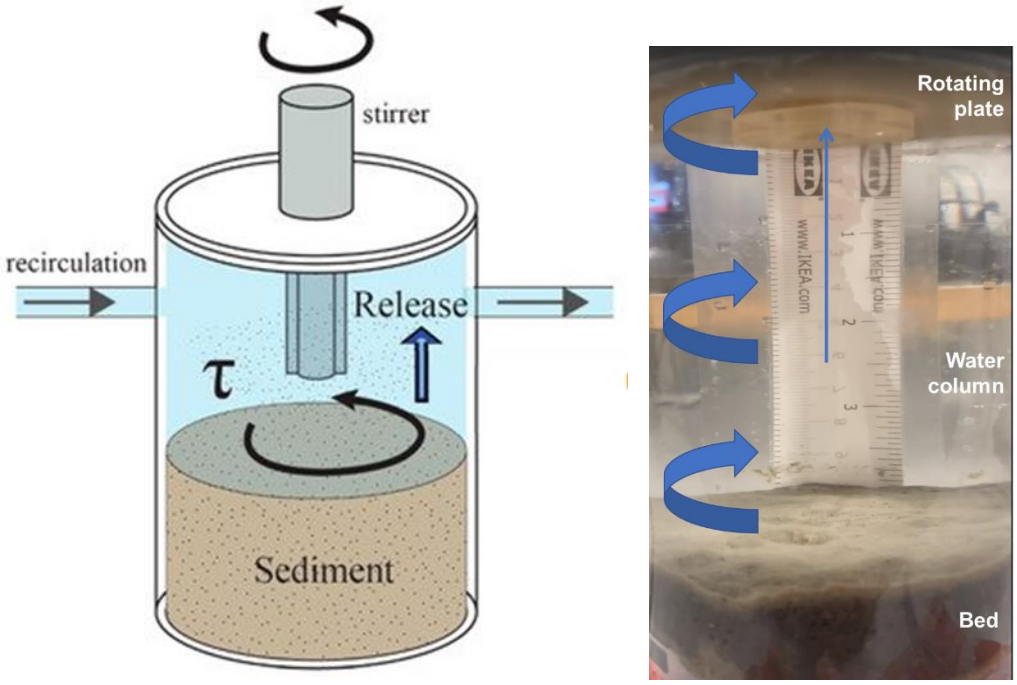

Figure 2-2 Set-up gust chamber. This device was used to study the erosion behavior at low uniform shear strengths: 0 - 0.65 Pa. Left schematic is adopted from Ding et al. (2019).

2.3.2 Rotational bucket

As the gust chamber cannot expose the gel to shear stresses beyond 0.65 Pa, a second simple improvised measurement device was created impromptu to test the gels' (micro) stability at higher shear stresses. It has been named a "rotational bucket" and it covers a range between roughly 0.4 – 1.8 Pa.

The setup exposes the gel to a shear stress by moving it through – ideally stagnant – water. It is assumed that this gives an erosion threshold in the same order of magnitude as a setup where the water is moved over the gel. It must be stressed that this test is merely conducted to get a feeling for the order of magnitude of the erosion threshold.

Figure 2-3 shows the setup of the rotational bucket. An aluminum cup containing the gel is attached to a wooden plate that is hold up by two metal wires (right panel). These wires are connected to an arm that rotates with help of an industrial mixer (left panel). Only the cup and bottom half of the wires are submerged as the water should not move along with the gel sample. The bucket is filled with tap water.

Figure 2-3 Set-up rotational bucket. This improvised set-up was used to estimate the erosion behavior for shear strengths beyond the range of the gust chamber (>0.65Pa).

An underwater GoPro camera (moving along with the sample) is used to study the gel stability for different rotational velocities. Each test is initialized in a stagnant bucket of water. Ultimately the water will rotate in the direction of the sample, which reduces the relative velocity and thus the shear stress experienced by the gel. Therefore, only the initial response of the gel is studied just after starting the rotation.

The tests are conducted at 6 different velocities for the 100, 200 and 400 Pa gel. This results in 18 tests in total. The maximum relative velocity experienced by the gel is varied between 0.44 and 0.9 m/s by varying the mixer's rotation speed. Based on the formulations by Soulsby (1997) for complex (non depth-averaged) flows (Equation 1), it is approximated that this amounts to flow-induced shear stresses between 0.42 and 1.77 Pa.

$$\tau_{flow} = \rho_{water}\, C\, U_{\mathrm{n.b.}}^2 \qquad \text{(Equation 1)}$$

In this equation, the shear stress is related to the flow velocity $[m/s]$ near the bed ($U_{n.b.}$) instead of the depth-averaged velocity. A dimensionless friction coefficient C [-] of 0.0022 is used, which is advised for smooth muddy bottoms.

2.4 Large-scale numerical model

The Delft3D sediment transport model developed from the Operationeel Stromingsmodel Rotterdam (OSR) NSC model is used to study the representative flow conditions and sedimentation in the port of Rotterdam. The Delft3D model has previously been used in the TKI PRISMA I study and the Sediment Trap Efficacy study. We refer to Cronin et al. (2021) for a complete overview of the model settings and performance.

2.4.1 Model description

The OSR-NSC model covers the Port of Rotterdam, a section of the North Sea near the Haringvliet and Maasmond and roughly 50 km upstream from the river mouth (Figure 2-4). The influence of tide, wind, waves, surge and density differences (due to gradients in salinity or sediment concentration) on the flow are accounted for. Three sediment fractions are included in the model, as well as a fluff and buffer layer for sedimentation van Kessel et al. (2007). The boundary and initial conditions are obtained from the larger OSR-Harbor model (Kirichek, et al., 2021).

The three-dimensional model consists of 20 sigma-layers in the vertical dimension. Its horizontal grid is curvilinear and has a standard resolution of 50 m. A higher resolution of 25 m is implemented in the most important harbor basins (Maasvlakte, Calandkanaal, 3rd Petroleum and Botlek, see Figure 2-4).

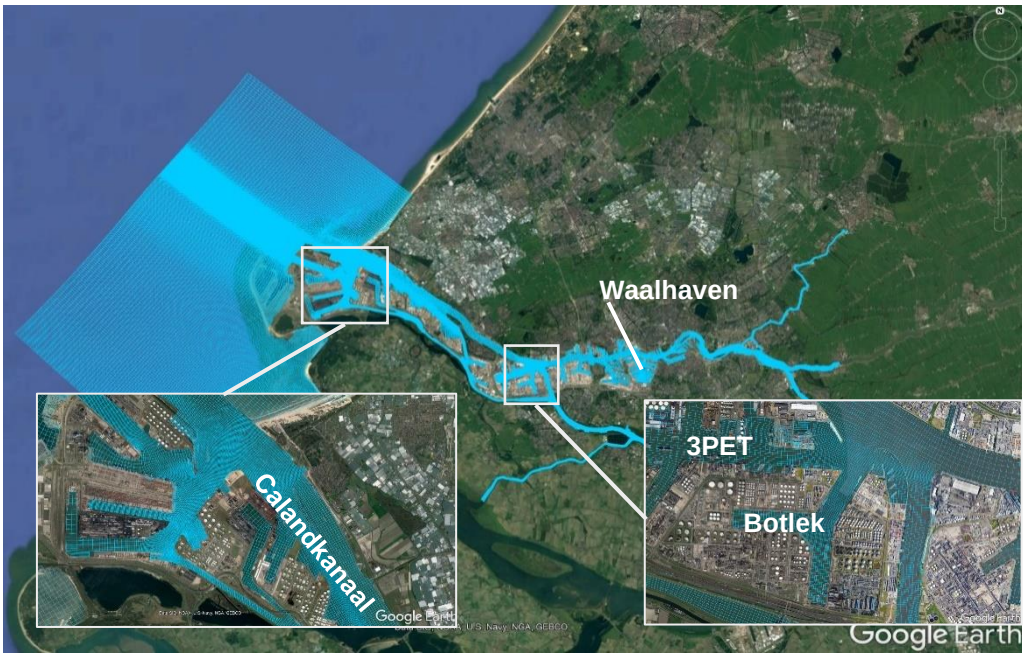

Figure 2-4 Model domain and curvilinear grid of the OSR-Harbor model in Delft3D. In Botlek/3PET, Calandkanaal and the Waalhaven, the model has a horizontal grid resolution of 25, 25 and 50 m, respectively.

Following Cronin et al. (2019), Kirichek et al. (2021) and Cronin et al. (2021), we simulate a spring-neap cycle in September 2016 which is intended to be representative for suspended sediment dynamics due to the average river discharge at Lobith and wind conditions.

2.4.2 Simulations

Apart from the reference simulation (without gel barriers), we simulate several scenarios with different barrier heights (1, 2, 3, 4, 5, 6m). This range is rather wide and the highest values are perhaps not practically feasible. It is done to approximate the gel barrier's potential to reduce sedimentation in the port and to assess the sensitivity of sedimentation to the barrier height. The gel barrier is implemented over the full width of the entrance of the Waalhaven, Botlek + 3rd Petroleumhaven and the Calandkanaal (Figure 2-5).

In the six simulations with six different barrier-heights, we simultaneously implement the barrier at all three locations. This is done under the assumption that there is little interaction

between the different harbor basins on the time scale of a spring-neap cycle. To test this hypothesis, a seventh simulation is conducted where a 3 m height barrier is implemented at the entrance Botlek + 3rd Petroleumhaven only. This allows us to study whether a decrease in sedimentation in one basin leads to an increase in sedimentation in another basin. To study where the sediment settles, we distinguish between 12 different sedimentation areas ('baggervakken') in the PoR (Figure 2-5). In the basins with a barrier, the baggervakken only include the area at the harbor-side of the barrier and exclude the area near the entrance (see zoomed-in box plots in Figure 2-5).

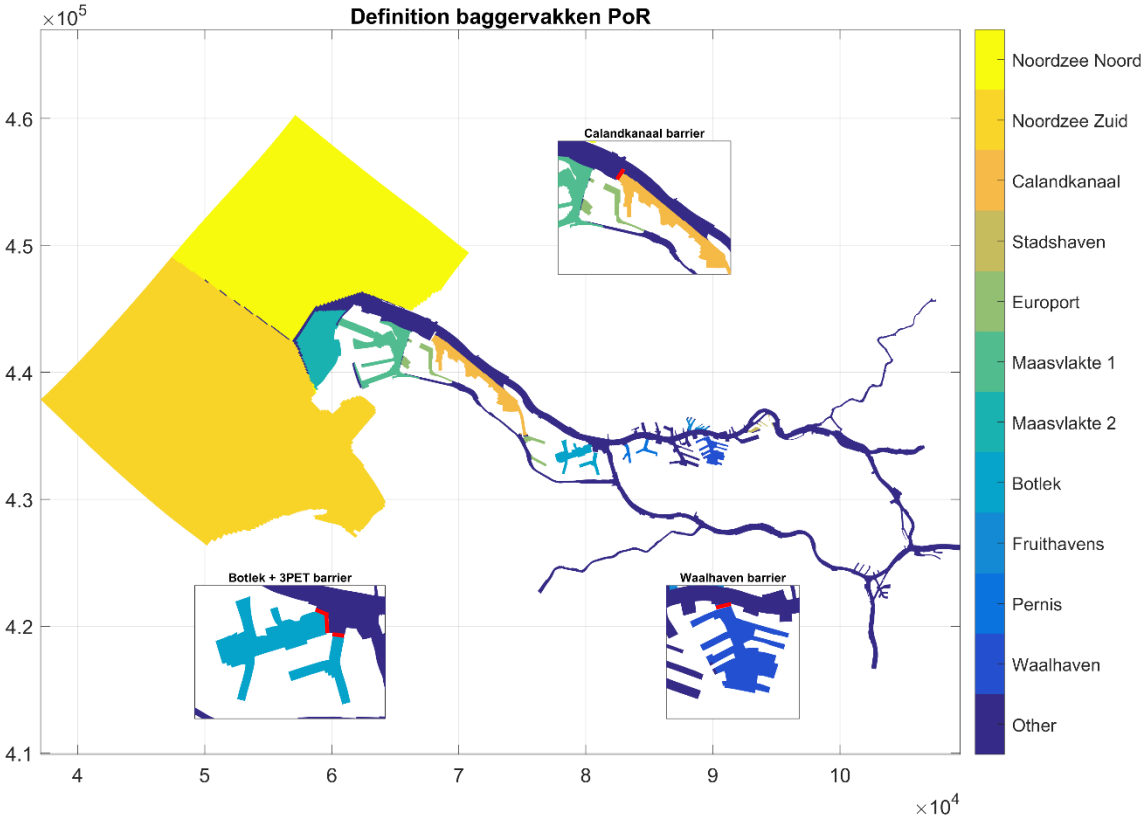

Figure 2-5 Barrier locations and definition of different sedimentation areas in the OSR-Harbor model ("baggervakken"). These areas are used to quantify sedimentation after a spring-neap cycle. Barriers are indicated in red. "Calandkanaal" also includes the Europoort harbors which are connected to the Calandkanaal.

The barriers are implemented in the model as rigid bathymetric features and therefore they remain intact regardless of the flow conditions. This implies that we are assessing a "best-case scenario" in terms of sedimentation reduction.

All barriers have a constant width of 100 m, which amounts to 4 cells in Botlek, 3rd Petroleumhaven, Calandkanaal and only 2 cells in the Waalhaven (Figure 2-6).

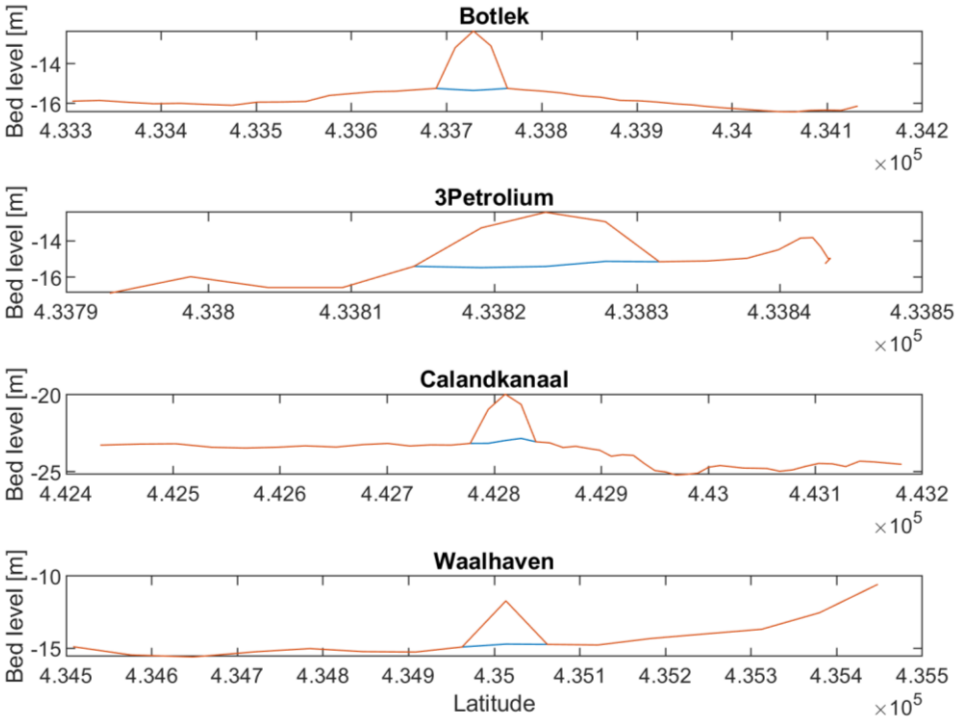

Figure 2-6 Cross-sections of 3 m-heigh barriers implemented in the bathymetry. Blue and orange lines indicate the original and adopted bathymetry, respectively. The width of the barrier is 100m, which amounts to 4 cells in Botlek, 3rd Petroleumhaven, Calandkanaal and only 2 cells in the Waalhaven.

2.5 CFD model

TUDflow3D is used to get a first indication on how the barrier behaves under the influence of the propeller of a sailing vessel.

2.5.1 Introduction

TUDflow3d is an open source 3D multiphase, variable density CFD (Computational Fluid Dynamics) model (https://github.com/openearth/tudflow3d) and has originally been developed for accurate near field simulations of TSHD (Trailing Suction Hopper Dredger) overflow plumes including the influence of the ship's propellers (de Wit, 2015). TUDflow3D has also been used previously to simulate near-field WID (water injection dredging) density currents in the Port of Rotterdam area (Kirichek et al., 2021; Cronin et al., 2021).

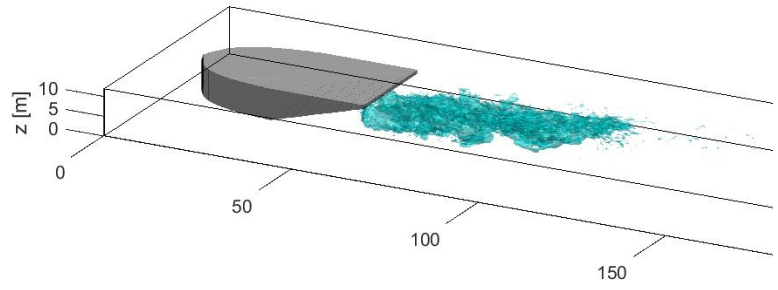

Figure 2-7 Schematic of a duo-propeller jet behind a schematic short ship hull in TUDflow3D.

TUDflow3d solves the non-hydrostatic 3D Navier Stokes flow equations including the influence of variable density. The influence of turbulence is captured by the Large Eddy Simulation approach in which the large turbulent eddies are resolved on the grid. The

influence of rheology is simulated by applying the apparent viscosity approach in combination with the often-used Papanastasiou regularization of the Bingham model. See ten Brummelhuis (2021) for more information about the implementation of rheology in TUDflow3D. The propeller jet is implemented in the CFD model with a rotating actuator disk approach (de Wit, 2015).

2.5.2 Model domain

In this study, we model the single propeller jet of a tanker in a basin with a comparable depth to the Botlek basin (16 m). The effective depth is 14 m, as the bottom two meters of the basin are assumed to be filled with the gel. The vertical resolution is 0.146 m, and the horizontal resolution varies between Δx=0.25-0.79m and Δy=0.25-0.71m (Figure 2-8). The maximum resolution is maintained in the region near the propeller where the turbulence is not yet fully developed. The lateral boundaries are closed. To allow for an efficient grid organization the vessel and propeller are stationary in position in the CFD model. The forward movement of the vessel is simulated by introducing an inflowing velocity, constant over the vertical without shear. This setup is numerically identical to a moving ship hull in stagnant water.

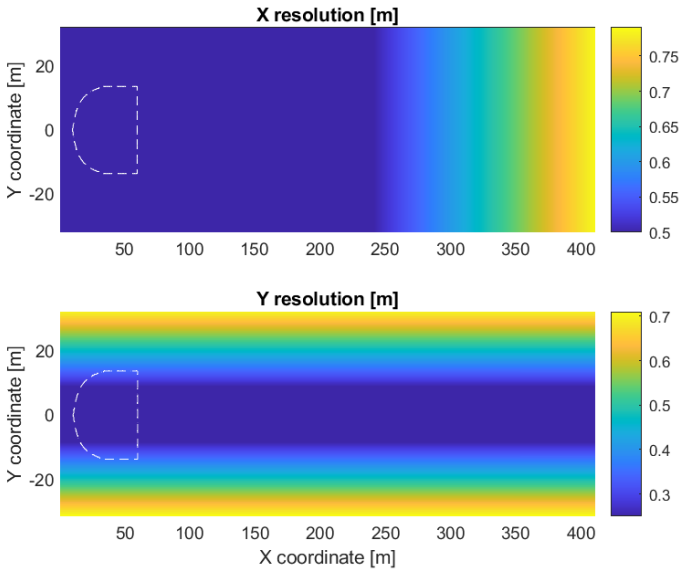

Figure 2-8 CFD domain resolution. Dotted line indicates the location of the vessel, the propeller of which is directed to the right.

2.5.3 Propeller jet

The propeller jet is modelled based on two vessel sizes. The characteristics of the vessels and its operations are selected in consultation with experts of PoR. The first is expected to enter the Botlek harbor every few days based on AIS data [1] and has a Dead Weight Tonnage (DWT) of ~ 80 kton. The second is the maximum size vessel that can enter the Botlek harbor since the deepening of the Nieuwe Waterweg, 3rd Petroleum harbor and Botlek in 2019 (~160 kton DWT). From now on, these vessels are referred to as the "representative" and "maximum" size vessel, respectively. To be economically feasible, the barrier should be able to withstand the exposure by a representative size vessel, whereas the exposure by the maximum size vessel is used as a worst-case scenario.

[1] AIS data for period from 6-10 until 7-10-2022 on marinetraffic.com. Visited 7-10-2022.

The propeller jets are modelled for 30% of the average power capacity of these vessels, as they are expected only to sail “half ahead” in the entrance of a harbor basin. According to the PIANC guidelines for scour protection (2015), this is a conservative figure with an exceedance probability of 5%. This amounts to 3 and 4.2 MW for the representative and maximum size vessel, respectively (Man Diesel & Turbo, 2014).
Based on the engine power and PIANC formulation (their equation 5-13), the propeller diameter is estimated to be 4.6 and 5.4 m for the representative and maximum size vessel, respectively (PIANC, 2015). A similar diameter is found when using the CUR Rock manual approach (propeller diameter $\approx 0.65 *$ draught).

To understand if the simulated propeller jet velocities are in the right order of magnitude, the CFD results are compared to the analytical solution in PIANC (2015) for non-ducted propellers (Dutch approach):

$$u(x,r) = 2\frac{u_0}{x/d}\, e^{-15.4\left(\frac{r}{x}\right)^2} \quad \textit{Equation 2}$$

$$u_0 = 1.48\left(\frac{P}{\rho d^2}\right)^{0.33} \quad \textit{Equation 3}$$

Where ρ is the water density, d is the propeller diameter, P is the used engine power, and where x and r are the downstream and radial outward direction, respectively. It must be noticed that this is the turbulence averaged solution that holds for an undisturbed propeller jet (i.e. without interaction with the quay walls and bottom). Although a rudder in the center behind a propeller causes more vertical diversion of the propeller flow, its influence is neglected in this analysis. For a sailing ship the analytical near-bed velocities are reduced by 0.5*Vship (Schiereck, 2019). In the simulations a forward vessel speed of 2 m/s is used, which is based on AIS observations in Botlek and Waalhaven on October 7th, 2022.

2.5.4 Rheology

With the CFD model, an attempt is made to simulate the non-Newtonian behavior of the gel under the influence of the propeller jet.

To do this, the gel is modeled as a Bingham fluid with a yield stress of $100\ Pa$ and a mixture density of $1100\ kg/m^3$. The Papanastasiou viscosity regularization is used with a m-factor of 2000. When the gel concentration falls below 90% of its initial concentration, the gel loses its Bingham yield strength in the model. This is based on small-scale experiments that indicate the gel disintegrates and loses strength as a result. The disintegration into disconnected gel chunks teared apart itself is impossible to model without using a very complex material model. But these numerical gel settings are selected after a sensitivity study to arrive at bulk gel erosive behavior in the CFD model as close as possible to the observed gel erosive behavior in the experiments. The final result of the sensitivity analysis is shown in Section 3.2

CFD simulations with a gel barrier of finite width over which a vessel is sailing turned out to be not stable. It falls outside present scope to fix this within this project. Therefore, instead CFD simulations of a vessel sailing over an infinitely wide gel barrier are presented.

Before simulating the gel's behavior under the influence of a propeller jet (Section 4.2), the CFD model’s ability to reproduce the experimentally determined erosion thresholds is verified (Section 3.2).

3 Gel stability

The stability of the gel is studied to test what flow conditions the gel can endure.

3.1 Lab experiments

First, we study the stability of the gel with lab experiments.

3.1.1 Gust chamber

The gust chamber is used to study the gel behavior for bed shear stresses between 0 and 0.65 Pa.

The experiments conducted in the gust chamber suggest that the gels (BYS = 100-400 Pa) do not erode for uniform bed shear stresses below 0.65 Pa. Only a few flocs that were already eroded during the infilling of the gust chamber, could be identified in the water column during the experiments (Figure 3-1).

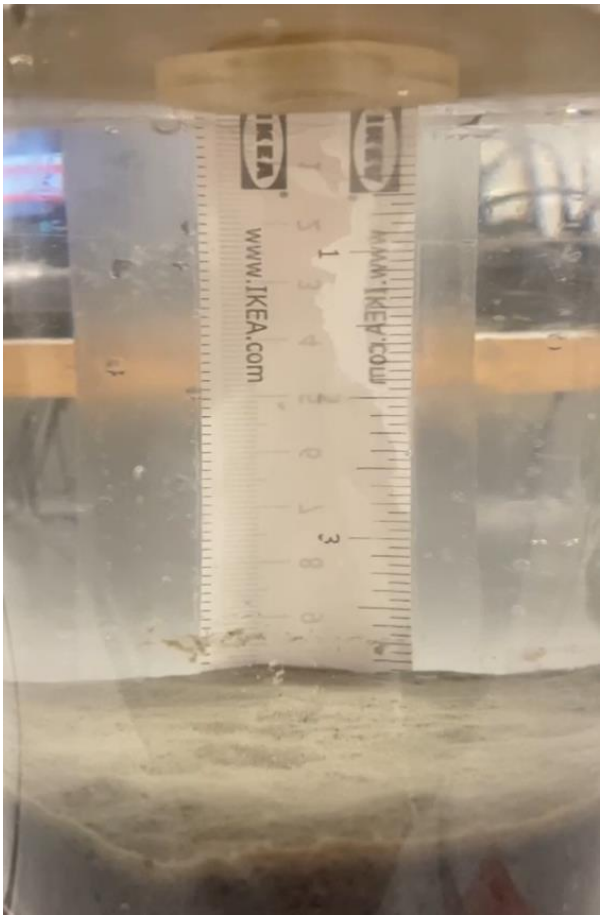

Figure 3-1 The "100 Pa Bingham yield stress"-gel remains stable for a flow induced shear stress of 0.65 Pa.

3.1.2 Rotational bucket

The rotational bucket is used to study the gel behavior for bed shear stresses above 0.65 Pa.

Figure 3-2 shows the gels' behavior for different flow velocities or shear stresses in an experiment matrix. The three columns indicate the gel with a Bingham yield strength of 100, 200 and 400 Pa, respectively. The six rows indicate the six flow velocities (shear stresses) to which the gels have been exposed, ranging between 0.44 m/s (0.42 Pa) and 0.9 m/s (1.77 Pa). The experiments were erosion is first identified are marked in red.

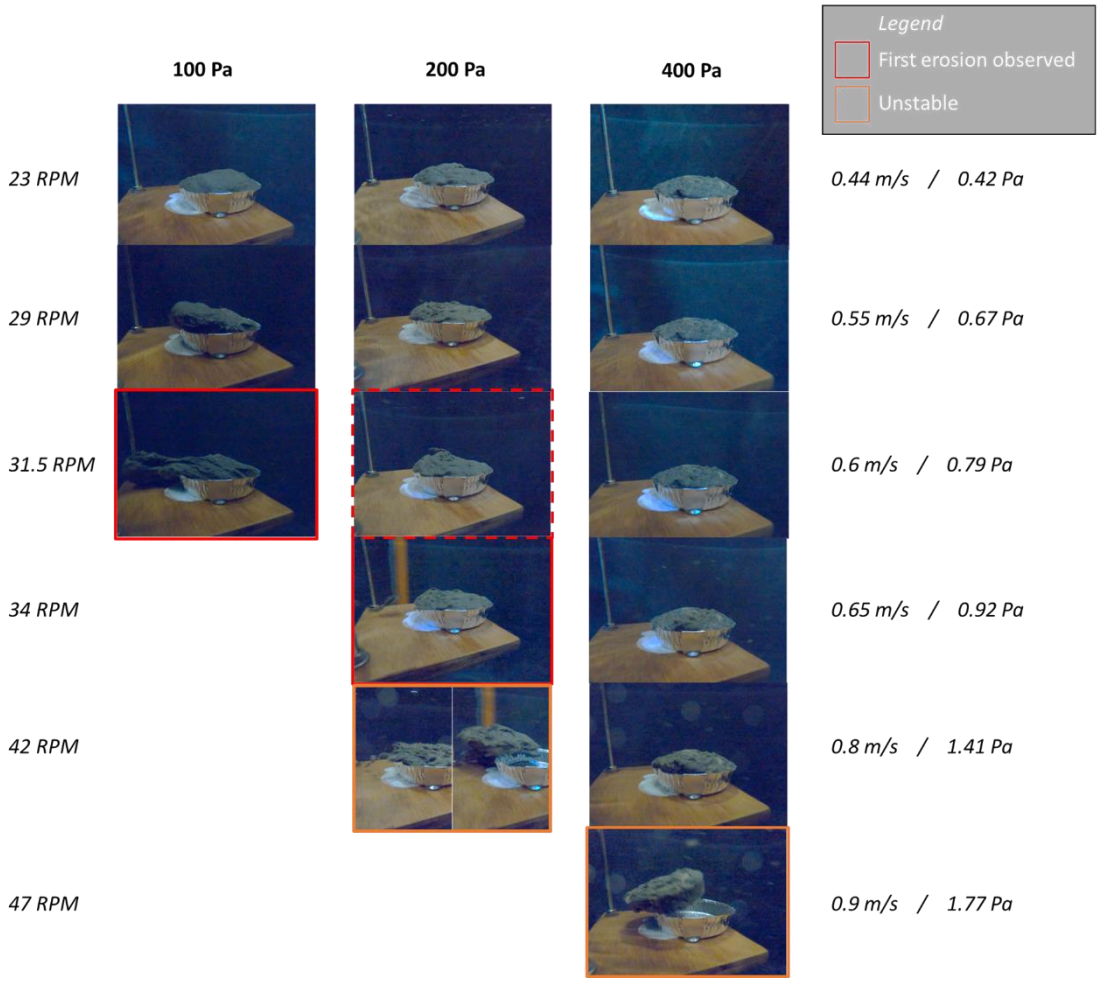

Figure 3-2 Experiment-matrix indicating the gels' behavior for different flow conditions. Columns indicate the three gels with a Bingham yield strength of 100, 200 and 400 Pa, respectively. Rows show experiments with different flow velocities / bed shear stresses. Every image shows a representative moment during the respective experiment. The velocities at which the first erosion is observed (i.e. the erosion threshold) are indicated with a red edge. The velocities at which the samples start to roll are indicated with an orange edge. The measured rotations-per-minute (RPM) are indicated on the left-hand side of each row. From the RPM, the flow velocity and bed shear stress are approximated (right-hand side).

In agreement with the Gust chamber, all gels remain stable for shear stresses below 0.67 Pa (0.55 m/s). At these velocities, the 100 and 200 Pa BYS gels vibrate while remaining stable (i.e. in their elastic phase). At roughly 0.8 Pa, the 100 Pa BYS gel starts showing plastic deformation. Chunks of 100 Pa BYS gel are detached periodically. This process resembles flow-like behavior rather than classical floc erosion (third row left column, Figure 3-2).

The stiffer 200 Pa BYS gel (middle column, Figure 3-2) starts showing floc-erosion like behavior when the flow shear stress is increased to 0.92 Pa (micro-instability). At a flow-induced shear stress of 1.4 Pa, the gel sample tumbles and is ejected from the cup (macro-instability). The stiffest 400 Pa BYS gel (right column, Figure 3-2) does not erode for flow shear stresses up to 1.41 Pa and is ejected from its cup at a shear stress of 1.77 Pa. For this gel, an erosion threshold cannot be assessed with the present setup. The tumbling and ejecting of the gel sample from the cup is not an erosion failure mechanism, but a macro-stability failure which is no topic for this study but important to consider in a follow up.

3.2 CFD results: erosion threshold

We test the ability of the CFD model to reproduce the erosion threshold of the gel in line with the experimentally determined threshold with the rotational bucket (Figure 3-2).

The flow velocity and Bingham Yield Strength (BYS) are varied in the input of the CFD model to approximate the conditions in the rotational bucket experiment. In agreement with the lab experiments, not much is happening for the 100 Pa BYS simulation when U=0.4 m/s and gel only starts to flow away from the top of the gel at U=0.6 m/s (Figure 3-3).

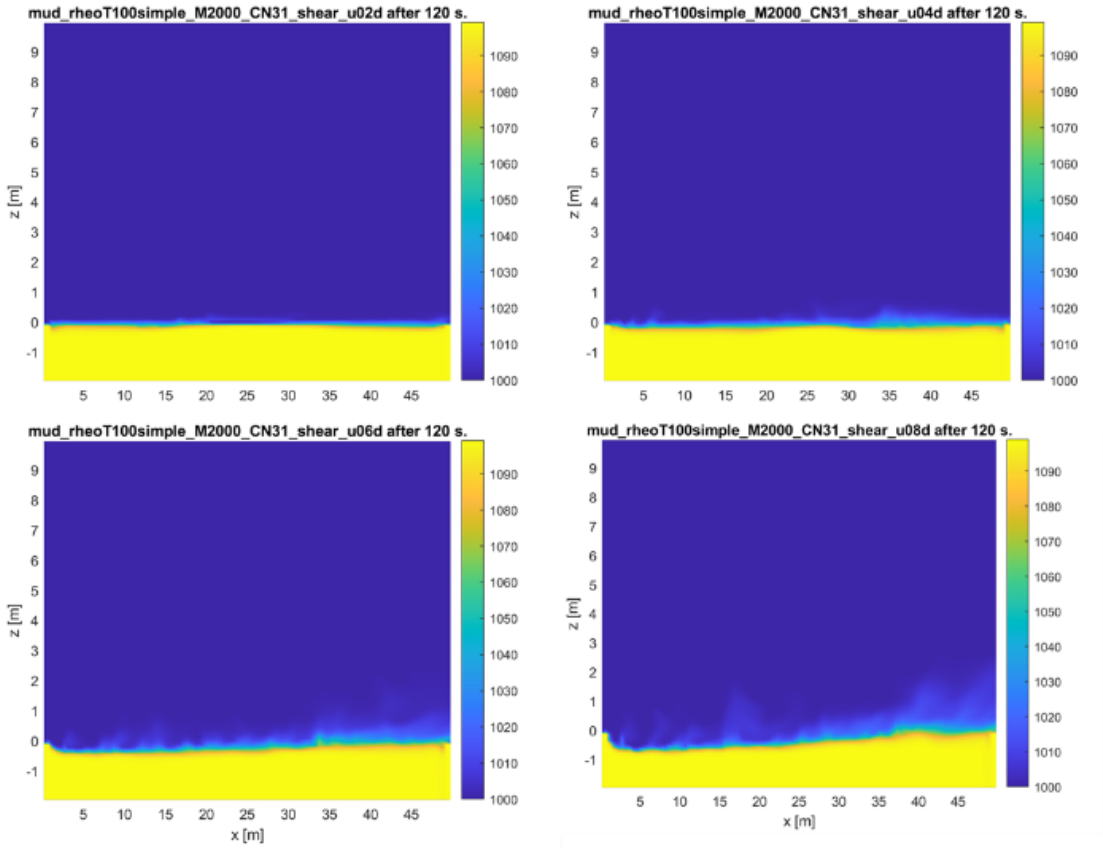

Figure 3-3 CFD simulation of a 100 Pa gel with a current of respectively 0.2, 0.4, 0.6, 0.8 m/s (top left to bottom right) flowing over it. The yellow color indicates the density which is an indication of the presence of gel.

For 200 Pa BYS simulation, the initiation of erosion is delayed to higher velocities (~0.8 m/s) (Figure 3-4). Finally, for 400Pa simulations no gel flows away from the top also at 0.8 m/s

(Figure 3-5). This is in agreement with the experimentally determined erosion thresholds in Figure 3-2.

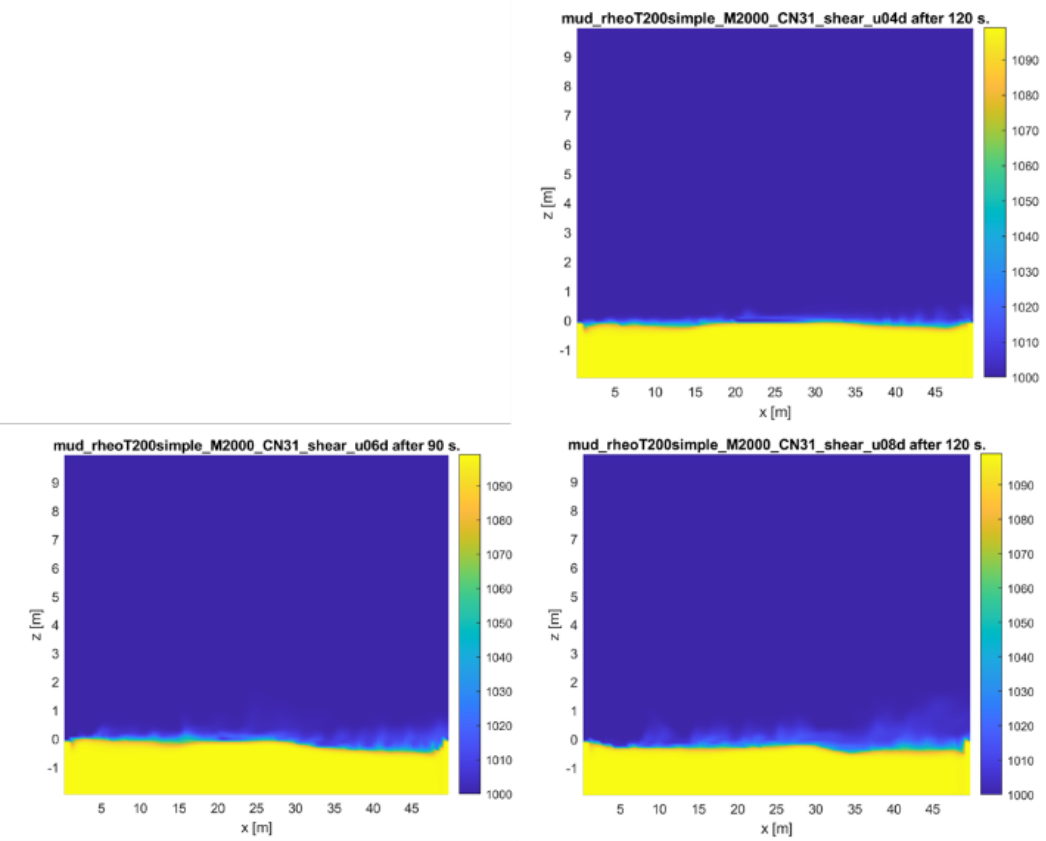

Figure 3-4 CFD simulation of a 200 Pa gel with a current of respectively 0.4, 0.6, 0.8 m/s (top to bottom right) flowing over it. The yellow color indicates the density which is an indication of the presence of gel.

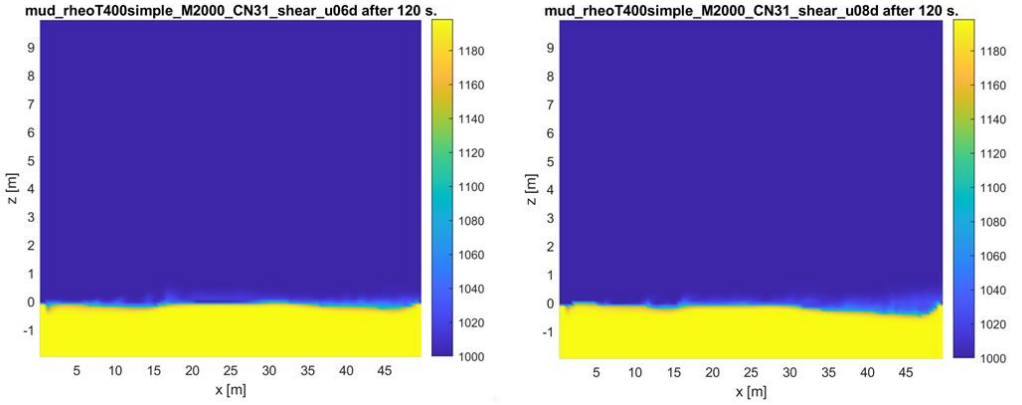

Figure 3-5 CFD simulation of a 400 Pa gel with a current of respectively 0.6 m/s (left) and 0.8 m/s (right) flowing over it. The yellow color indicates the density which is an indication of the presence of gel.

3.3 Discussion

The lab experiments were initiated to get insight into the gels' erosion thresholds. The experimental gust chamber and rotational bucket results suggest that the gels are not eroded for shear stresses below +/- 0.8-0.9 Pa. This amounts to near-bed flow velocities of roughly 0.6 m/s for which the gel remains intact.

3.3.1 Erosion threshold

It must be stressed that the experimental setup used in this study, is not meant to give a precise erosion threshold but rather an order of magnitude estimate. One of the difficulties in precisely determining an erosion threshold, is that the water in the rotational bucket cannot fully be prevented from rotating along with the gel sample and the go-pro. This could result in lower relative flow velocities and therefore less erosion. In the set-up centrifugal forces play a role. In addition, the bed shear stress formulation by Soulsby (1997) for complex (non depth-averaged) flows is associated with considerable uncertainty. Nevertheless, it is reassuring that the outcomes from the rotational bucket test and the gust chamber are not in contradiction but in line with each other: both experiments show that no erosion occurs for shear stresses below 0.65 Pa.

The results in Figure 3-2 indicate that the gels' erosion thresholds are 2 orders of magnitude smaller compared to their Bingham yield stress (BYS). That is ~ 0.8 and 0.9 Pa for the 100 and 200 Pa BYS gels, respectively. An erosion threshold which is two orders of magnitude smaller than their BYS was also found by van Kessel et al. (2021) who show that the erosion threshold of freshly deposited mud beds is two orders of magnitude smaller than their BYS.

The gels' erosion behavior differs however, considerably from the erosion behavior of muddy beds. First, the visually observed vibrations of the material suggest that the gels behave elastically up to relatively large strain rates. Furthermore, fresh gels do not diffuse but rather loose chunks of material. While for the 200 Pa BYS gel this occurs in form of floc erosion, the 100 Pa BYS gel first deforms plastically ('flows') and then tears. For the stiffest gel (400 Pa BYS) an erosion threshold is not identified, as it remains stable for velocities up to 0.9 m/s (1.8 Pa) after which it is ejected from its cup.

3.3.2 Other failure mechanisms

In Phase 1 of this study swelling was identified as a time-dependent mechanism. This can form a failure mechanism as swollen gel has a low strength and will be peeled off from the barrier by currents, after which the next layer will swell (etc.). Small-scale experiments in Phase 1 showed that this process occurs at a rate of 1-2 cm per day, see Figure 3-6 (top-left). Assuming this rate is scale-independent, this would imply a lifetime of 100 days for a 1 m-heigh gel barrier (based on the current gel recipe).

The experiments of Phase 2 have not only shed light on the order of magnitude of the gel's erosion threshold, but also on several additional failure mechanisms (Figure 3-6). Floc erosion is identified as a surface process that affects the gel. In terms of macro-instability, both flow behavior and the rolling/translating of a gel barrier are identified in the experiment and they could form a possible failure mechanism. The latter could imply that a barrier could tumble or be pushed away if its weight and/or friction with its subsurface are not sufficient. In the experiment the gel patch was initially hold in the cup at all side edges which will not be the case for a gel barrier in the port and still it was lifted outside the cup and tumbled. A possible remediation for this failure mechanism is to increase the density of the gel or the extra height in a real gel barrier might add sufficient weight to withstand this mechanism in a

full-scale application. These additional failure mechanisms are not investigated further in this study, but it is recommended to include them in a follow-up study.

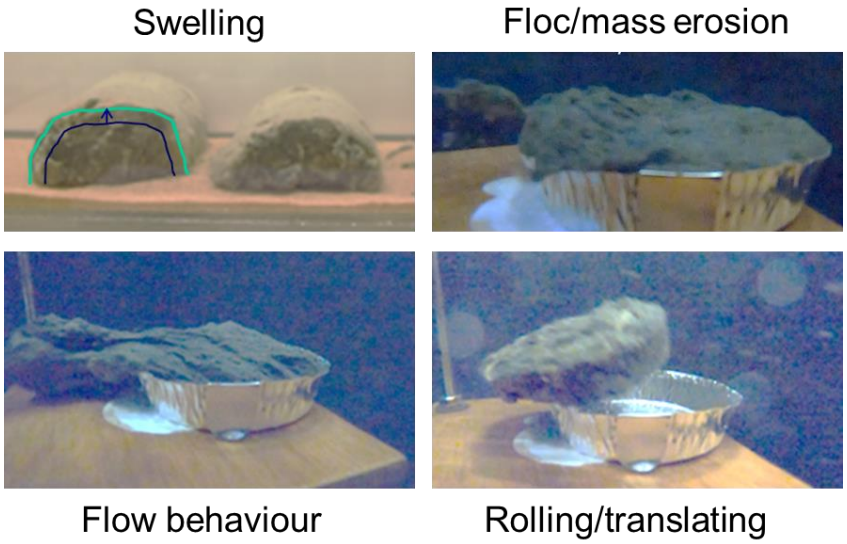

Figure 3-6 Failure mechanisms for Xanthan Gum based gels. Micro-instability: swelling, erosion. Macro-instability: flow deformation, rolling/translating.

3.3.3 Knowledge gaps

The erosion threshold of the 400 Pa BYS gel might be identified if the velocity could be increased without the gel sample being ejected from the cup. This could be achieved by increasing the friction in the aluminum cup or by scaling-up the experiment to increase the mass of the gel sample.

Larger scale experiments (e.g. in a flume) could also give more insight on the gels' macro stability. If the translating of the gel appears to be important even at a large scale, it makes more sense to assess the gel's stability in terms of drag and density instead of only looking at surface erosion by bed shear stress. Finally, for safety reasons, it would be interesting to assess how easy it is for ships to sail through a barrier. At the present scale, we observe that even the stiffest (400 Pa BYS) gel is easily compressible with a finger.

The present results are not conclusive yet on what failure mechanism is dominant and thus directive for the longevity of a barrier. The placement method of the gel, its age and time-dependent characteristics, its frictional resistance with the subsurface and the salinity of the water are expected to be important conditions that could influence the swelling, erosion, plastic deformation and translating of the gel (and thus its longevity).

Based on the findings of present work, this section can be seen as suggestions on gel stability topics to investigate further in a follow up study.

4 Gel stability for PoR flow conditions

This chapter investigates whether the gel is likely to remain stable under flow conditions in the Port of Rotterdam. To this end, the ambient flow conditions in the PoR are simulated using a Delft3D model and compared to the experimentally determined erosion threshold (Section 4.1). In addition, TUDflow3D simulations are used to study whether propeller jet-induced currents would exceed the gel's erosion threshold. This gives insight in the most promising locations to construct a gel barrier in terms of stability.

4.1 D3D results: natural flow conditions

We simulate a complete spring-neap cycle in May 2016 to study the flow conditions throughout the Port of Rotterdam (PoR). Five locations where a gel barrier could be useful are examined based on the Delft3D model results (Figure 4-1).

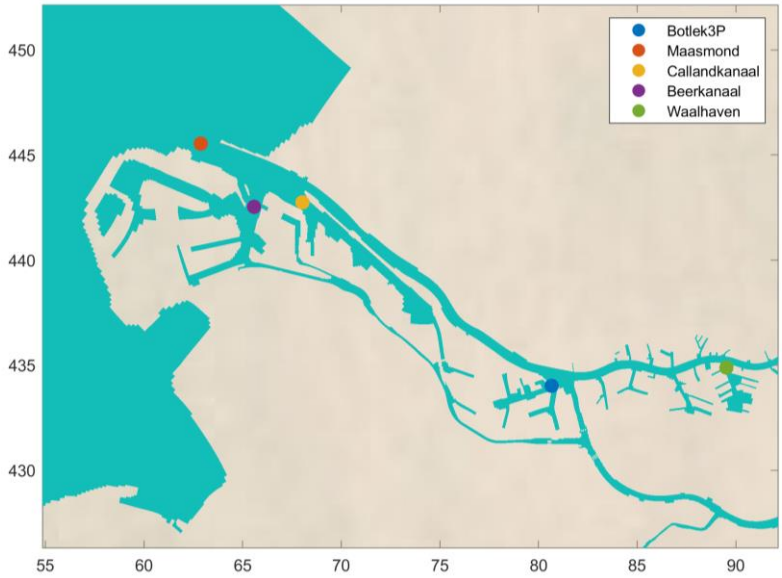

Figure 4-1 Five locations in the Port of Rotterdam where a gel barrier could be placed, and where the flow conditions are studied in this chapter.

4.1.1 Qualitative description

First, we qualitatively describe the flow conditions in the basins where the barrier could be constructed.

Figure 4-2 and Figure 4-3 show a prototypical 2DV velocity and salinity profile at the Maasmond and the entrance of Botlek, respectively. In the river mouth (Maasmond) and inland harbors (Waalhaven, Botlek and the 3rd Petroleum) the highest velocities are caused by an exchange flow, where the surface and near-bottom velocities are in opposite direction. This is true for both neap and spring tide. The highest near-bottom velocities at the Maasmond occur before/around high-water (red shades left panel) and are associated with high-salinity waters entering the Nieuwe Waterweg (yellow shades right panel). A few hours later, after high-water, the highest near-bottom velocities occur at Botlek. These too are associated with high-salinity water entering the basin near the bottom. At Botlek, however, both the velocity magnitude and salinity are attenuated compared to the Maasmond.

At the Beerkanaal and Calandkanaal, the flow field is more erratic and therefore more difficult to describe qualitatively. Here too, the flow velocities near the surface and bottom can be in opposite direction. Typical near-bed velocities in Beerkanaal and Calandkanaal are 0.5 m/s.

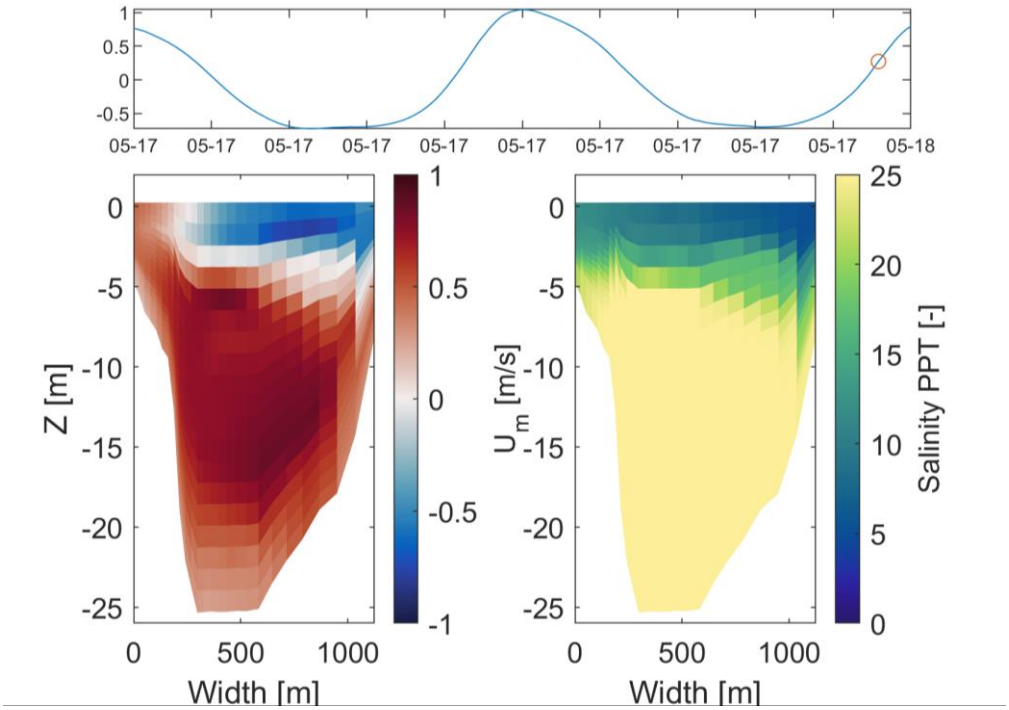

Figure 4-2 Prototypical 2DV velocity and salinity profile near the river mouth (Maasmond) at the phase of the tide with maximum near-bed flow (indicated with the red circle in the top panel). Left panel shows the velocity profile, where red denotes water entering the river and blue shades denote water flowing into the sea. Right shows salinity in parts-per-thousand.

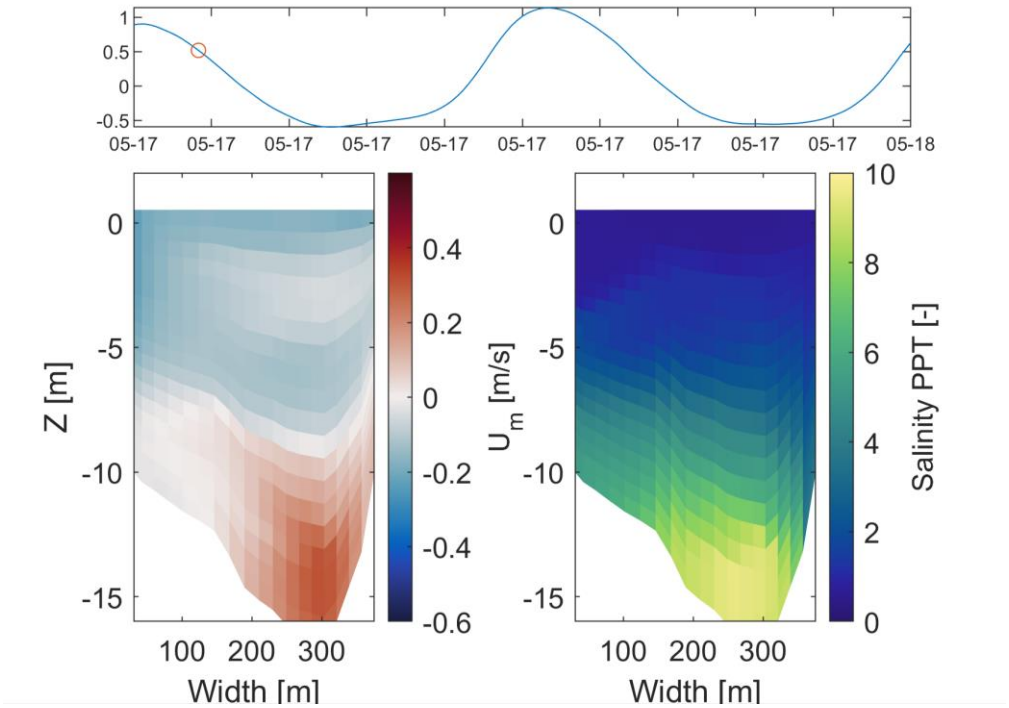

Figure 4-3 Prototypical 2DV velocity and salinity profile at the phase of the tide with maximum near-bed flow (indicated with the red circle in the top panel) further upstream, at Botlek.

4.1.2 Exceedance of erosion threshold

At the selected locations in the Port of Rotterdam (Figure 4-1), bed shear stresses are studied. For each harbor basin, it is approximated how frequently the experimentally determined erosion threshold is exceeded during the simulated spring-neap cycle.

Figure 4-4 to Figure 4-8, show the cumulative occurrence probability of bed shear stress during the studied spring-neap cycle at five locations in the PoR. The green vertical line indicates the upper shear stress limit of the calibrated Gust chamber, for which no erosion was identified (i.e. < 0.65 Pa). The gray vertical line is the erosion threshold of the “100 Pa BYS gel”, which was approximated with the improvised rotational bucket experiment (i.e. ~0.8 Pa). Erosion is not expected to occur in the region left of the green line, whereas it is expected to occur in the region to the right of the gray line. The results per location are summarized in Table 4-1.

The results indicate that bed shear stresses at Botlek/3Pet (Figure 4-6), Waalhaven (Figure 4-7) and Calandkanaal (Figure 4-8) do not exceed the 0.8 Pa erosion threshold during the simulated spring-neap cycle. In fact, bed shear stresses at these locations remain below the maximum shear stress which could be achieved with the calibrated Gust chamber (for which the gel did not erode). This suggests that these are promising locations for the construction of a gel barrier in terms of micro-stability.

At Maasmond (Figure 4-4) and Beerkanaal (Figure 4-5), the experimental rotational bucket erosion threshold is exceeded for at least 7 and 1% of the time, respectively (see intersect gray and blue lines). Here, shear stresses only remain below the upper limit of the Gust chamber for 90 and 98% of the time (see intersect green and blue line). In other words, erosion is not expected to occur at these locations for *at least* 90 and 98% of the duration of the simulated spring-neap cycle (Gust chamber threshold), and *probably* for about 93 and 99% of the time (based on the rotational bucket threshold).

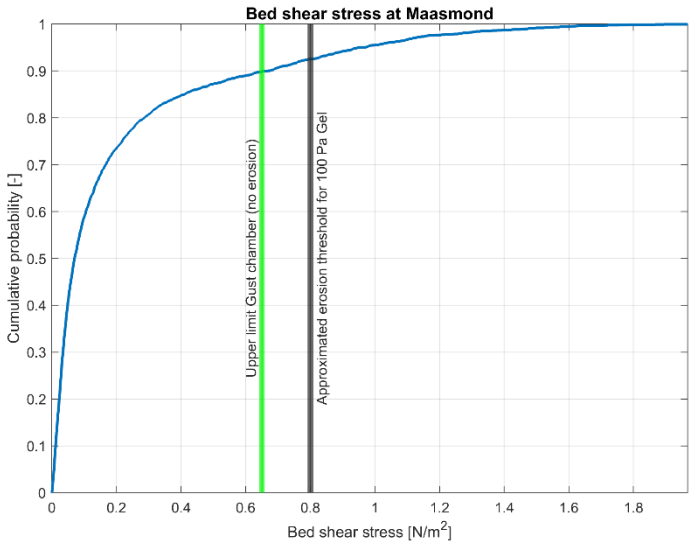

Figure 4-4 Cumulative probability of bed shear stresses occurring at the Maasmond river mouth during the simulated spring-neap cycle in Delft3D. Green vertical line shows the upper shear stress limit of the calibrated Gust chamber (i.e. 0.65 Pa), for which no erosion was identified. Grey vertical line shows the erosion threshold for the 100 Pa BYS gel (i.e. 0.8 Pa), which was approximated with the improvised rotational bucket experiment.

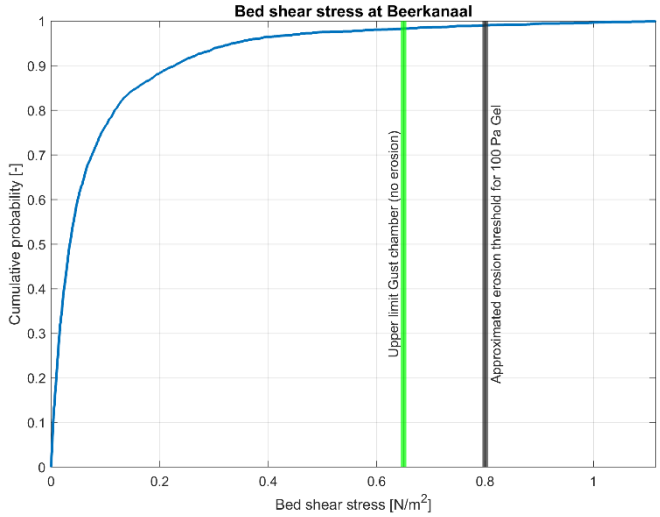

Figure 4-5 *Cumulative probability of bed shear stresses occurring at the entrance of the Beerkanaal during the simulated spring-neap cycle in Delft3D.*

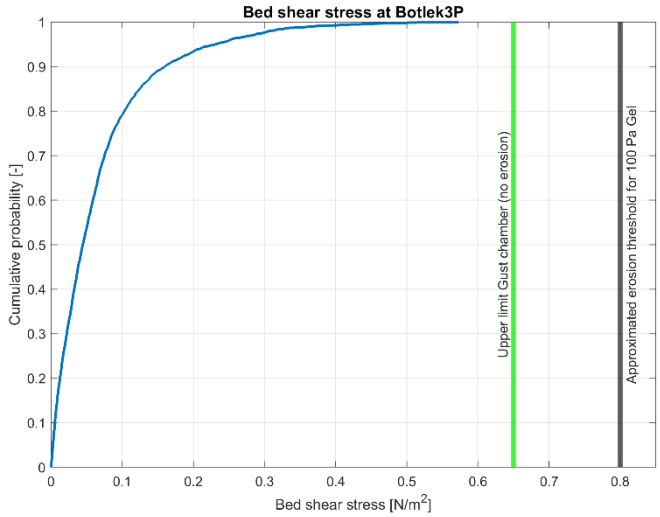

Figure 4-6 Cumulative probability of bed shear stresses occurring at the entrance of the Botlek harbor basin during the simulated spring-neap cycle in Delft3D.

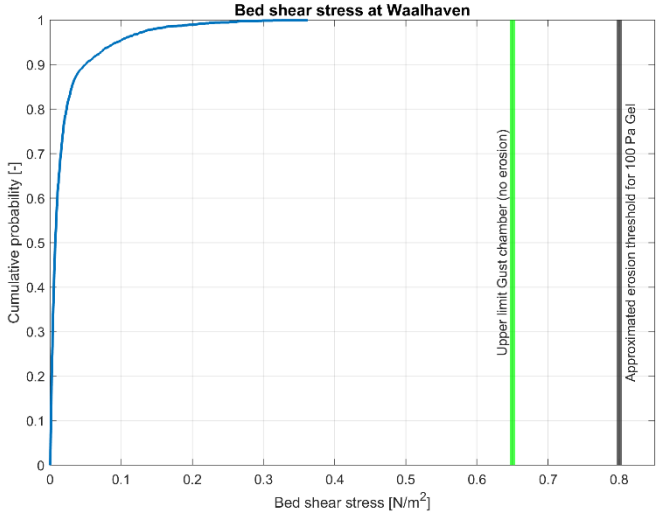

Figure 4-7 Cumulative probability of bed shear stresses occurring at the entrance of the Waalhaven harbor basin during the simulated spring-neap cycle in Delft3D.

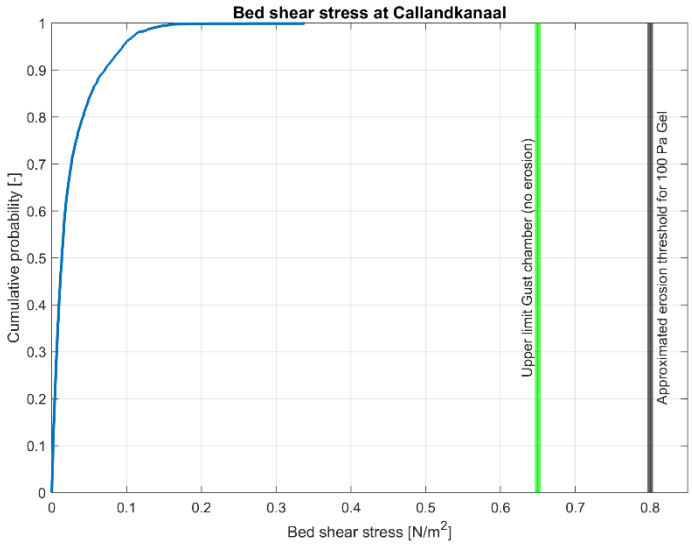

Figure 4-8 Cumulative probability of bed shear stresses occurring at the entrance of the Calandkanaal during the simulated spring-neap cycle in Delft3D.

Table 4-1 99th-Percentile bed shear stresses throughout the Port of Rotterdam during the studied spring-neap cycle. Green values do not exceed the erosion threshold of the 100 Pa BYS gel, which was approximated to be ~ 0.8 Pa based on the rotational bucket experiment.

Location	τ_{P99} $[Pa]$	% Time exceeding erosion threshold
Maasmond	1.6	7%
Beerkanaal	0.9	1%
Botlek / 3rd Petroleum	0.5	0%
Waalhaven	0.25	0%
Calandkanaal	0.2	0%

4.2 CFD Results: propeller jet exposure

CFD simulations are used to get a first indication on the flow exposure and damage realized by the propeller of a large vessel that is representative for entering Botlek and by the propeller of the maximum size vessel that can enter Botlek.

4.2.1 Qualitative description

The propeller jets are simulated and described for four different under keel clearances (UKC): 0, 2, and 4 m. This are indications of the velocities a gel barrier will face when the reference ship is sailing over the gel barrier with a gap of 0, 2, and 4 m (Figure 4-9) between the top of the gel barrier and the keel.

In the simulations with a 2 and 4 m UKC, the core of the propeller jet is drawn towards the surface of the basin. In the simulation with a 0 m UKC, the propeller jet remains attached to the bottom for a while. For a small UKC, the flow is accelerated around the ship which strongly influences the flow field and jet (bottom row, Figure 4-9).

The influence of engine power on the jet strength (compare columns Figure 4-9) is small compared to the influence of the UKC (compare different rows). The reason might be that the larger propeller diameter of the larger vessel partly mitigates the effect of the larger engine power on the jet strength.

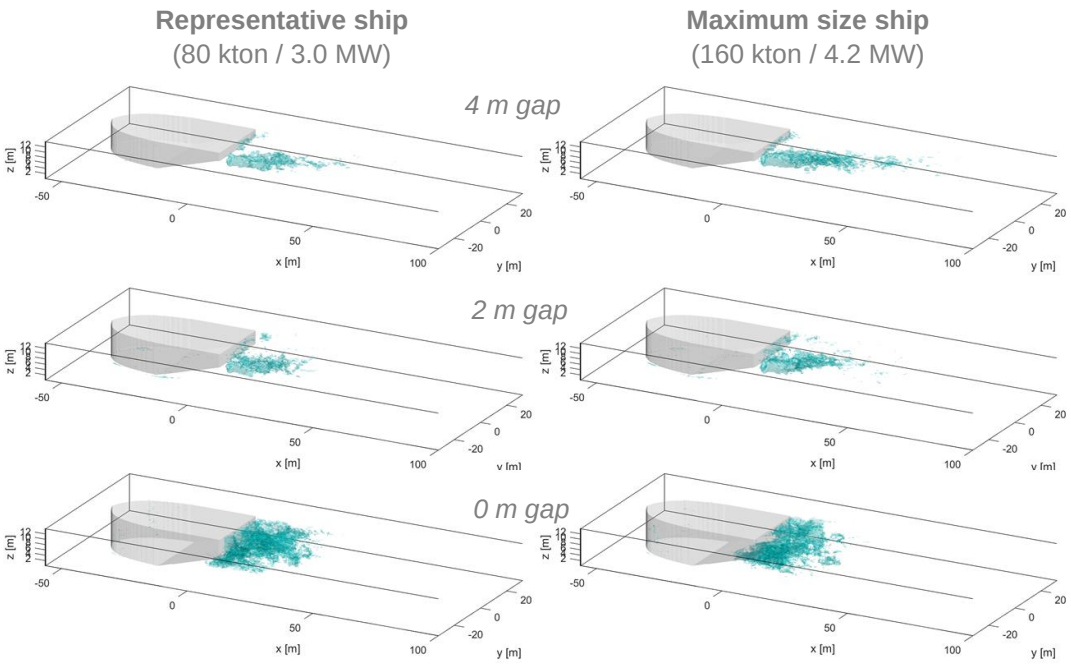

Figure 4-9 Propeller jets for different under keel clearances (UKC) (0, 2, 4 and 6 m). UKC is the gap between the bottom of the vessel and the bottom of the basin. The propeller tip is aligned with the bottom of the ship. Left images show the propeller of a large ship that is expected to enter Botlek every few days (sailing at 30% of the average power = 3 MW). Right images show the propeller of the maximum size vessel that could enter Botlek (30% power=4.2MW). Jets are visualized by indicating the contour with a velocity of 3.4 m/s (relative to the bottom).

4.2.2 Exceedance of erosion threshold

To assess if the currents generated by the propeller exceed the erosion threshold, near bed velocities are studied for different UKC based on the CFD simulations and an analytical solution. The ships are assumed to sail half ahead at a velocity of 2 m/s.

Figure 4-10 and Figure 4-11 show the results for the representative and maximum size vessel at Botlek, respectively. Notice that the analytical results are turbulence averaged (red line), whereas the CFD results are instantaneous at t = 50 seconds (blue line). As the influence of the bed and free surface on the propeller jet location and flow is not incorporated in the analytical solution, the resulting near-bed velocity profiles of the CFD simulations and analytical solution deviate from each other. Close to the propeller, for example, there are high near-bed velocities in the CFD results which are not visible in the analytical solution. They are caused by the approaching water flowing into the propeller and the flow acceleration around/underneath the ship.

Both the CFD and analytical results indicate that the experimental erosion threshold (~ 0.6 m/s for a 100 Pa BYS gel) is exceeded for a 0 and 2 m UKC whereas it is generally not exceeded for a 4 m UKC. The CFD results indicate that the turbulent fluctuations can be in the order of 1 m/s (noise in blue line). This suggests that single turbulent fluctuations could exceed the experimentally determined erosion threshold of 0.6 m/s, even for a 4 m UKC.

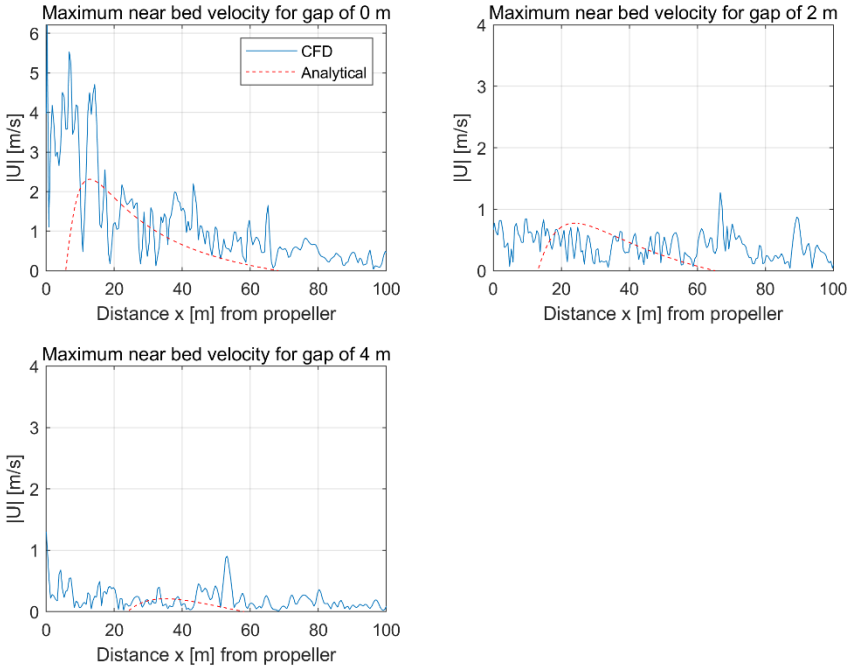

Figure 4-10 Near bed velocities generated by a propeller jet of a representative ship in Botlek, for different under keel clearances (UKC): 0, 2 and 4 m. Red lines indicate the velocity based on the analytical solution for an undisturbed jet in PIANC. Blue lines indicate the magnitude of the simulated near bed currents in TUDflow3D at y = 0m. The propeller is located at x=0m. Propeller jet velocities correspond to a large ship that is expected to sail in Botlek every few days (at 30% of the average power = 3 MW).

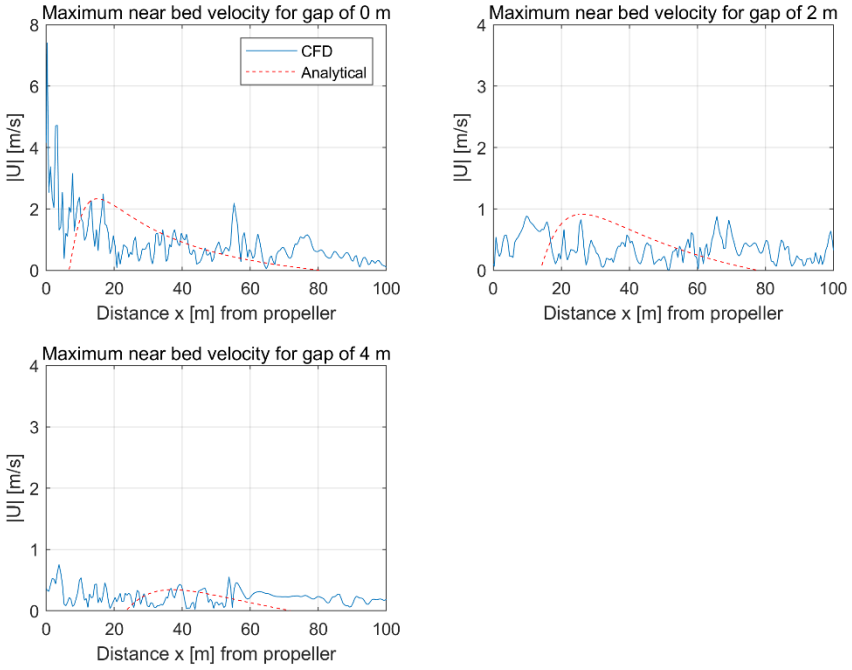

Figure 4-11 Near bed velocities generated by a propeller jet of the maximum ship size that can enter Botlek, for different under keel clearances (UKC): 0, 2 and 4 m. Propeller jet velocities correspond to the maximum size ship that could sail in Botlek (at 30% of the average power = 4.2 MW).

The spatial distribution of the near-bed propeller jet velocities is shown in Figures 4-12 and 4-13, for the representative and maximum size vessel at Botlek respectively. Both the analytical and CFD results indicate that for a gap of 2 m, the near-bed propeller flow velocities exceed the erosion threshold of 0.6 m/s. For a gap of 0 m between the gel barrier and ship, even velocities above 2 m/s can be expected (bottom rows Figures 4-12 and 4-13). For a UKC of 4 m, the erosion threshold is not exceeded in the turbulence averaged analytical result and only locally exceeded in the CFD result (top rows Figure 4-12 and 4-13).

These results show that the propeller jet velocities that a gel barrier would have to endure when a ship is passing are serious and could easily exceed the erosion threshold as determined in Section 3.1. This is especially true if the distance between the keel of the ship and the gel barrier is 0-2m.

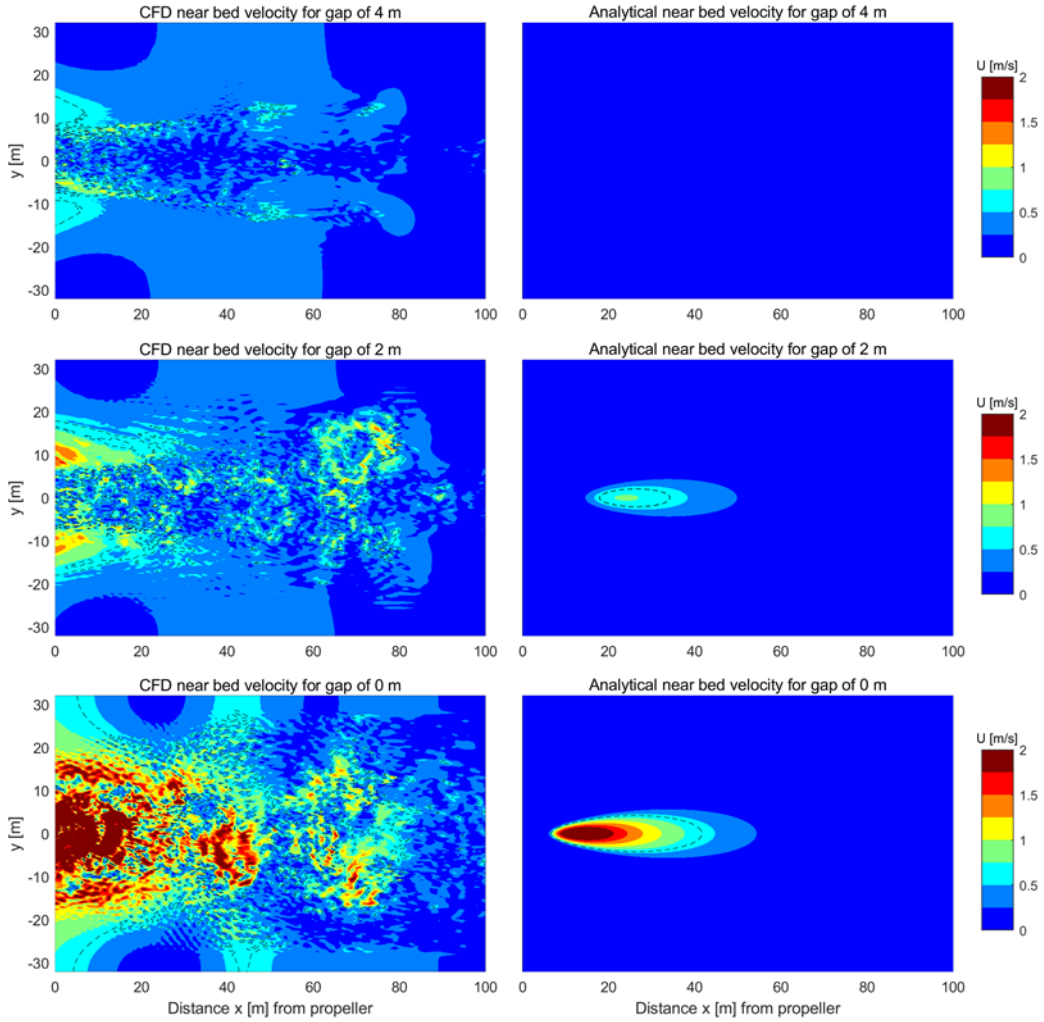

Figure 4-12 Spatial distribution of the near bed velocities generated by a propeller jet of a representative ship in Botlek, for different under keel clearances (UKC): 0, 2, 4 and 6 m. The black dashed contour indicates the 0.6 m/s velocity threshold for a gel barrier. Propeller jet velocities correspond to a ship that is expected to sail in Botlek every few days (at 30% of the average power = 3 MW).

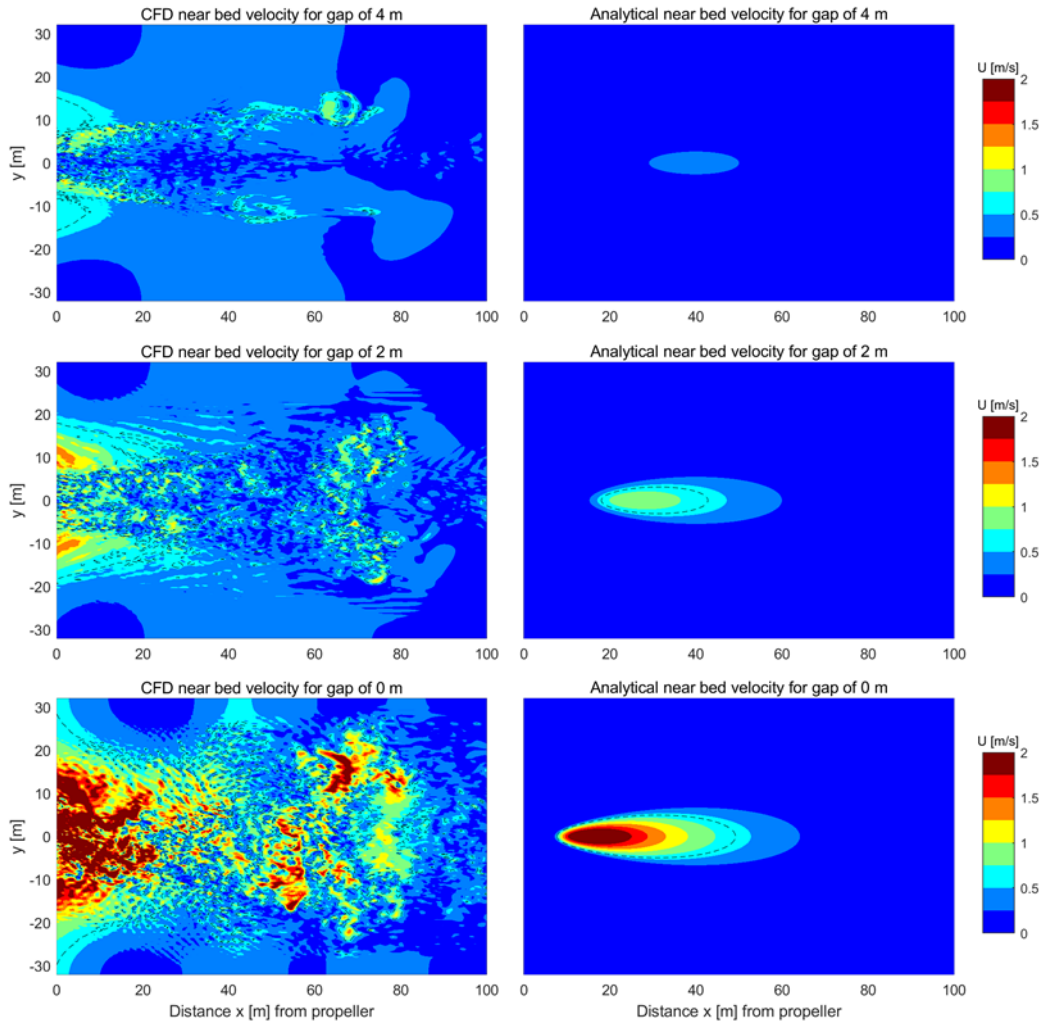

Figure 4-13 Spatial distribution of the near bed velocities generated by a propeller jet of the maximum size vessel that could enter Botlek, for different under keel clearances (UKC): 0, 2, 4 and 6 m. The black dashed contour indicates the 0.6 m/s velocity threshold for a gel barrier. Propeller jet velocities correspond to the maximum size ship that could sail in Botlek (at 30% of the average power = 4.2 MW).

4.2.3 Simulated damage to barrier

We use non-Newtonian Bingham CFD simulations to get a first indication of how the gel behaves under the influence of the propeller of a vessel. This is done based on the maximum size vessel that could enter Botlek (sailing at 30% of the average propulsion power = 4.2 MW).

Figure 4-14 shows what the initially 2-m thick gel layer with a 100 Pa BYS looks like after 50 s of the ship sailing over it with a sailing velocity of 2 m/s. At this speed a ship would sail over a 100 m wide gel barrier in 50 s. The gel initially covers the full numerical domain, as if the vessel is sailing over an infinitely wide barrier. This was done to ensure stability (see Section 2.5.4).

For a 4 m gap between gel and keel, the gel is not destroyed (top panel Figure 4-14). The gel underneath the propeller jet core is displaced (blue area) and moved outward with respect to the jet core (brown area). The indent and associated bumps in the gel travel at the speed of the vessel and the gel layer always maintains a certain thickness in time. This suggests that

the deformation of the 100 Pa gel layer (by a vessel with a 4 m gap from the top of the gel barrier) is not permanent. This is in agreement with the finding that the gel's erosion threshold is not exceeded for a 4 m gap found in the previous chapter.

For a 0 and 2 m gap, the 100 Pa gel is fully removed over a distance of > 10 m (bottom and middle panel Figure 4-14). Accordingly, in previous section the gel's erosion threshold of 0.6 m/s was found to be exceeded for these configurations (see Figure 4-13).

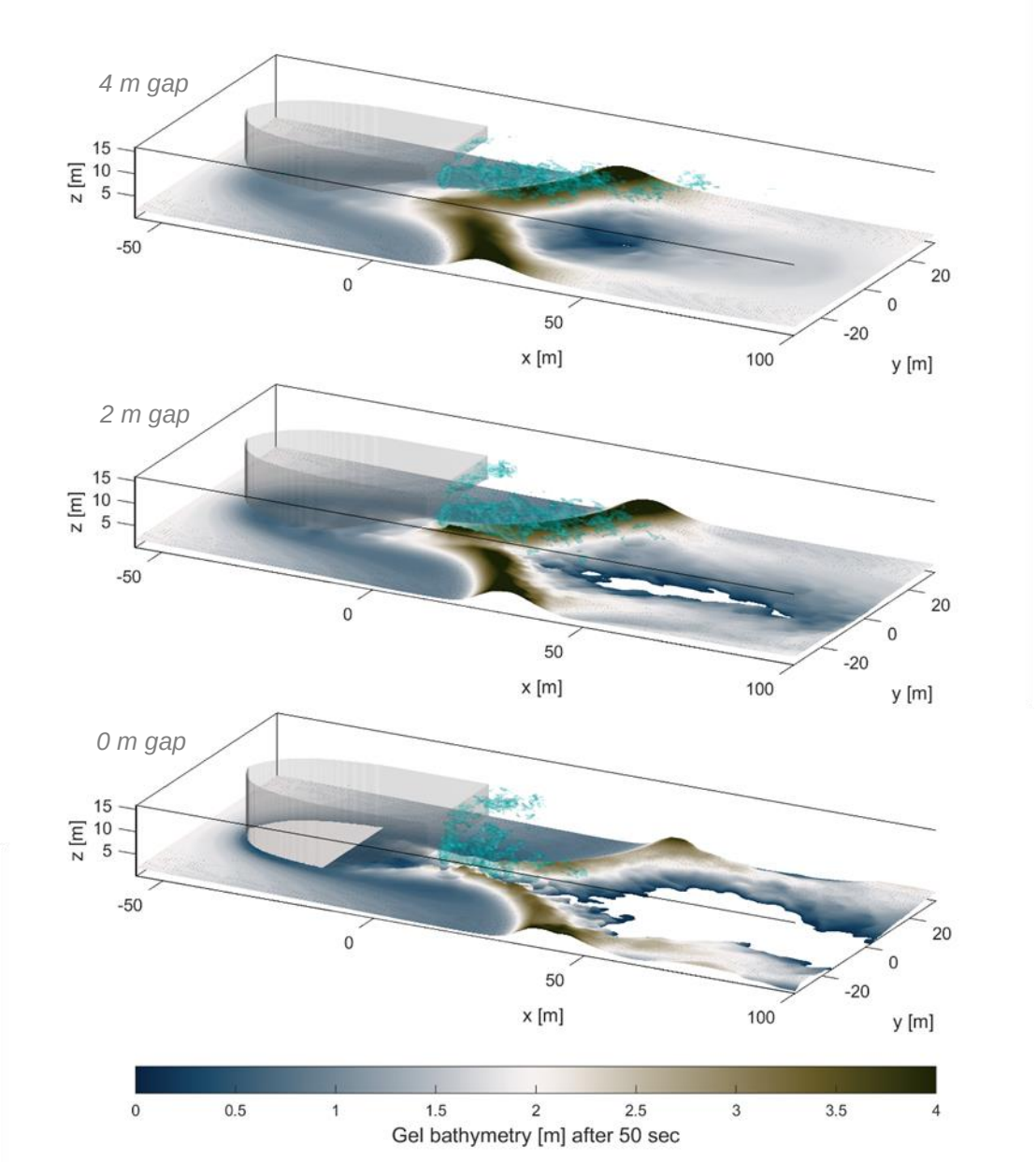

Figure 4-14 Gel barrier thickness after 50 seconds of sailing over an initially 2-m thick gel layer. The contour shows the location of the 90% value of the initial gel concentration, Brown and blue colors indicate where the gel layer thickness has increased and decreased, respectively. White areas indicate areas where the gel has been fully removed.

The gap where the gel is removed has a limited width for a 2 m gap (middle panel Figure 4-14). About 100 m behind the moving ship, the increased gel elevation at the lateral sides flows slowly back toward the center hole in the gel barrier (white gap). The average barrier gel height at 100 m behind the ship, however, is lower than the initial barrier height because

gel has eroded from the barrier during the simulation. In reality, the barrier has a limited width and it is possible that the recovery of the barrier hole is less than shown in this simulation with an infinite wide barrier over which the vessel is sailing.

4.3 Discussion

Delft3D and CFD simulations were initiated to assess if the gel's erosion threshold (as approximated in Chapter 3) is exceeded by natural and vessel-induced currents in the PoR, respectively.

The Delft3D results indicate that natural currents exceed the erosion threshold of the "100 Pa BYS"-gel in the Beerkanaal and Maasmond for roughly 1 and 7 % of the time. The results are more promising in the Calandkanaal, Botlek and 3rd Petroleum harbor, where natural currents always remain in the shear stress range for which no erosion is expected to occur based on the calibrated Gust chamber experiments. These inland harbors are deemed most suitable for the construction of a gel barrier (e.g. in a pilot). The CFD results suggest however, that even in these basins the erosion threshold might be exceeded by the propeller jet of vessels with a small gap of 0-2 m between the gel barrier and the keel.

4.3.1 Thinking in terms of erosion thresholds

In this chapter, the exposure which the gel would have to endure is studied in several locations in the PoR in terms of bed shear stress. The shear stresses are compared to the experimental benchmarks from chapter 3. It is important to realize however, that it might not be possible to fully describe gel's micro-stability in terms of uniform bed shear stresses. Drag, whirls and incidental peak velocities might also be important for the gel's stability, as well as the local strength properties of the gel which would - amongst others - depend on the gel's fabrication and placement method.

Finally, it must be noticed that the present results do not say anything about the feasibility of a gel barrier in terms of macro stability (e.g. failure by translating of the barrier).

4.3.2 Delft3D results: natural currents

Although an erosion rate is not presented in this study, it is expected that the exceedance of the erosion threshold at the Beerkanaal and Maasmond (with 1 and 7% of the time) would considerably limit the longevity of a barrier at these locations. Although at the Calandkanaal, Botlek and 3rd Petroleum, the erosion threshold is never exceeded during the simulated spring-neap cycle, certain sources of uncertainty must be discussed.

First, the (cumulative) bed shear stress results in Figure 4-4 to Figure 4-8 are taken from the Delft3D simulation without gel barriers. Gel barriers might, however, influence the flow which could result in higher bed shear stresses. Still the present approach is deemed reasonable, as test CFD simulations with and without a gel barrier showed little difference in the resulting bed shear stress.

Secondly, the (cumulative) bed shear stresses are based on a specific set of boundary conditions as we simulate a spring-neap cycle in September 2016.

4.3.3 CFD results: ship propeller jet currents

The CFD results indicate that the damage done by the propeller of a ship passing over a 100 Pa BYS gel barrier could be serious, especially for a small gap of 0-2m between the keel and the top of the gel barrier. Using a stronger gel could be a part of the solution, as the 400 Pa BYS gel for instance did not erode/deform for the tested velocities (< 0.9 m/s). However, more research on the navigability of stiffer gels would be required. Alternatively, it could be a PoR consideration to let vessels throttle down when crossing the barrier to minimize damage.

The studied set of conditions was selected based on expert judgement and correspondence with the PoR. More analysis is required on different combinations of sailing velocity, propeller power/diameter and gap between keel and gel barrier and on how frequently vessels with each characteristic can be expected in the PoR. Furthermore, some characteristics of a vessels and the harbor basin have not been considered whatsoever – such as the rudder. Rudders are known to partly deflect jets towards the bottom, resulting in higher near-bed velocities (and possibly more destruction). This is to some extent compensated by the relatively narrow schematization of the harbor basin (~60 m), as the lateral boundaries in the CFD model enhance the flow.

To get a first indication of how the gel behaves under the influence of the propeller of a vessel, the gel has been modelled as a Bingham fluid. The temporary deformation of the gel barrier under the influence of a vessel with a 4 m gap (top panel Figure 4-14), resembles the temporary deformation which is observed in the lab experiments for velocities below the erosion threshold (middle panel in Figure 4-15 below). For smaller gaps and velocities above the erosion threshold, the simulated gel barrier shows permanent damage (bottom and middle panel Figure 4-14). However, these results are indicative only because the gel is modelled as a Bingham liquid rather than a fully elastoplastic material which can tear into chunks, caution is advised when interpreting the damage.

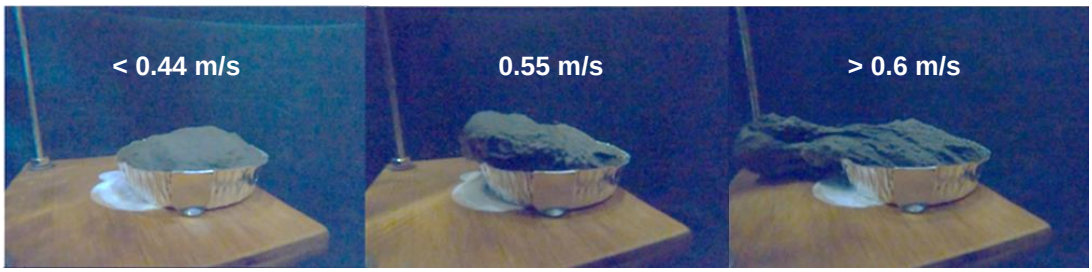

Figure 4-15 Response of 100 Pa BYS gel, which was used as a reference in the CFD simulation, for different flow velocities.

The CFD model may both overestimate and underestimate the gel barrier damage. In the model, the thickness of the modelled barrier is decreased due to dispersion of the gel into the water column. Furthermore, a gap is formed in the barrier under the core of the propeller jet. In the lab experiments, the gel never really disperses but shows plastic (permanent) deformation (right panel Figure 4-15). If the gel does not disperse but merely deforms, this might yield more favorable results compared to the CFD simulations (i.e. is if the deformed barrier remains functional). On the other hand, the CFD results might be too optimistic with respect to the restoring ability of the gel. In the simulation with a 2 m gap, the hole in the gel barrier underneath the propeller jet had a limited width and the gel at the lateral sides of the gap flowed back to the center hole (~100 m behind the ship, middle panel Figure 4-14). In the small-scale experiments, the gel does not recover its shape when it is sheared beyond the erosion threshold (right panel Figure 4-15). It is unclear to what extent the gel would really flow back into the gap once it has deformed plastically. Another difference is the finite width of a gel barrier over which a vessel is sailing vs. the unlimited width of the gel barrier in the model. In the model gel cannot be pushed out of the gel barrier at the edges, but in reality, this could happen.

5 Potential sedimentation reduction by gel barriers

For the three most promising locations in terms of stability, a large-scale hydrodynamic model is run to assess the potential sedimentation reduction. The associated annual savings in terms of dredging costs and emissions are estimated.

5.1 Overview

We compare the maximum sedimentation reduction in the Calandkanaal, Botlek/3rd Petroleum harbor and the Waalhaven.

Figure 5-1 gives an overview of the sedimentation reduction in the selected harbor basins for barrier heights varying between 0 and 6 m. For realistic barrier heights (<4m), the effectiveness of a gel barrier is negligible in the Calandkanaal (turquoise line). For the more inland harbors, the results are more promising. In the Waalhaven and Botlek, sedimentation reductions in the order of 5.8% (~20 ton/day) and 17% (~170 ton/day) are realized for a 3 m high barrier.

The sedimentation reduction does not appear to scale linearly with the barrier height. At Botlek, the sedimentation is decreasing more than linearly for barrier heights up to 3 m. At Waalhaven, the sedimentation continues to decrease more than linearly for barrier heights up to 6 m. Finally, at Calandkanaal, a decrease in sedimentation only becomes noticeable for barriers higher than 4 m.

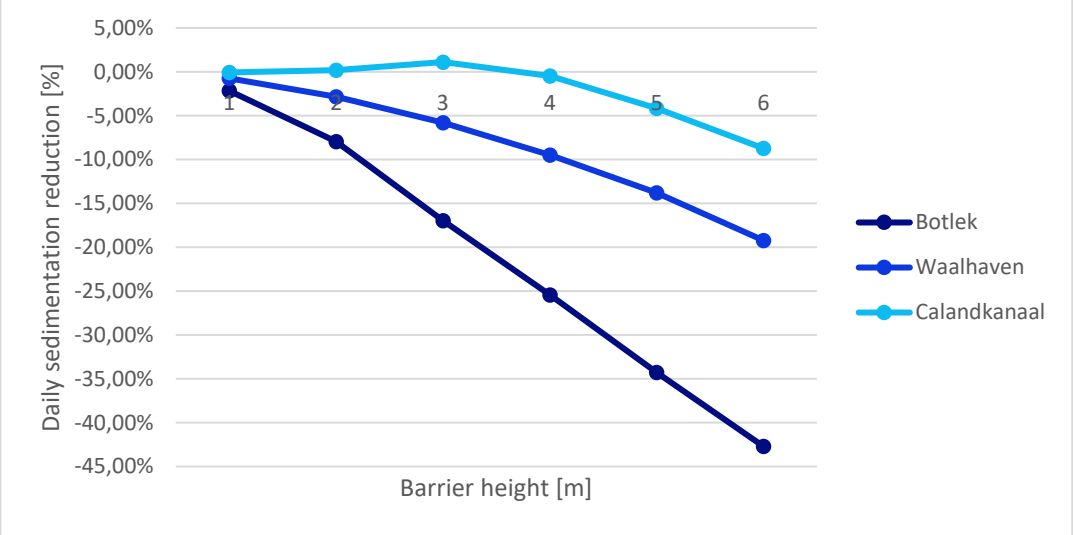

Figure 5-1 Potential sedimentation reduction per harbor basin for barrier heights between 1 and 6 m. Results are based on the Delft3D OSR-NSC model in which all barriers have been implemented simultaneously as rigid structures. Percentual decreases are relative to the reference simulation, without a barrier.

The reduction in sediment deposition seems to be related to the relative height of the barrier compared to the thickness of the bottom layer of the water column which carries most sediment (i.e. $H_{barrier}/H_{turbid}$).

In Botlek, the bottom layer of the water column with the highest sediment concentrations (> $0.03\ kg/m^3$) is roughly 1 m thick. This implies that the simulated barriers (1-6 m) are relatively high compared to the bottom layer of the water column that carries most sediment (i.e. $H_{barrier}/H_{turbid}$ > 1). Consequently, the barrier appears to be most effective in hampering sediment transport and reducing sedimentation in this basin.

At Calandkanaal, the layer of the water column with high sediment concentrations (> $0.03\ kg/m^3$) reaches relatively high in the water column compared to the tip of the barrier (i.e. $H_{barrier}/H_{turbid}$ < 1 for all barrier heights). In this basin, the barrier appears to be less effective hampering the sediment transport and reducing sedimentation in this basin.

Finally, at Waalhaven the bottom layer of the water column with high sediment concentrations (> $0.03\ kg/m^3$) is roughly 3 m thick. Here, the simulated barriers are roughly as high as the bottom layer of the water column that carries most sediment (i.e. $H_{barrier}/H_{turbid}$ ~ 1). This might contribute to the more than linear decrease in sedimentation for a higher barrier height. In addition, the barrier in Waalhaven is placed in a relatively low-lying area compared to the river and the harbor basin (see Figure 2-6). This might also contribute to the barrier at Waalhaven being less effective compared to the barrier in the Botlek.

For the three studied locations, the vertical distribution of suspended sediment is shown in Appendix A.2 for different barrier heights.

5.2 Analysis per harbor basin

Here, the sedimentation (patterns) and sediment exchange are studied per harbor basin.

5.2.1 Botlek & 3rd Petroleum

Table 5-1 shows the average sedimentation rate that is realized in the Botlek and 3rd Petroleum (3PET) harbor for different barrier heights. For a 3 m high barrier, for example, the sedimentation rate is reduced from 1011 to 839 ton/day (~ minus 170 ton/day).

Table 5-1 Sedimentation [ton/day] for different barrier heights in the entrance of Botlek/3PET.

Reference [ton/day]	1m barrier	2m barrier	3m barrier	4m barrier	5m barrier	6m barrier
1011	988 (-2.16%)	930 (-7.9%)	839 (-17.0%)	754 (-25.4%)	664 (-34.3%)	579 (-42.7%)

The results indicate that both the sediment flux in and out of Botlek and the adjacent 3rd Petroleum harbor are affected for different barrier heights. Both the inflow and outflow of sediment are reduced for a larger barrier height, which suggests that a higher barrier can also trap sediment which would otherwise be flushed out of a basin. This is visualized in Appendix A.1. This finding suggests that the barrier could also be used to reduce the spreading of contaminated sediments from certain harbor areas.

At Botlek, the net effect is a reduction in sediment import. For a 3 m heigh barrier, -1.33 kg/s less sediment enters the 3rd Petroleum and -0.63 kg/s less sediment enters Botlek. This amounts to roughly 170 ton/day less sediment entering the basins in total, which is in the same order of magnitude as the reduction in the sedimentation rate for a 3 m high barrier (Table 5-1: 839 - 1011 = -170 ton/day).

Figure 5-2 shows how the reduction in sedimentation is spatially distributed over the basin. The decrease in sedimentation is mostly observed in the direct proximity of the barrier and deeper in the basins at the end (blue shades). Interestingly, sedimentation even increases in a large part of the basin (red shades). Nevertheless, on a scale of a single harbor basin it seems that the required sailing distance to the offshore disposal area decreases as the sediment settles closer to the basin entrance. This may be favorable in terms of dredging costs or emissions.

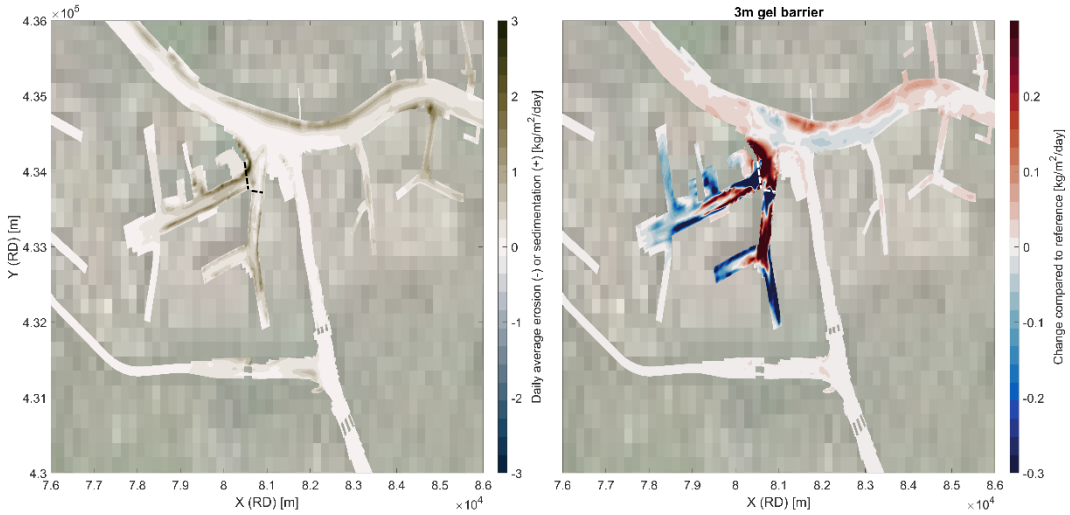

Figure 5-2 Change in spatial sedimentation patterns for a 3 m high barrier at Botlek and the 3rd Petroleum harbor. Left panel shows the daily average sedimentation rate in the simulation without a barrier. Right panel shows the relative increase/decrease in sedimentation rate for a 3 m high barrier. The approximate location of the barrier is indicated with the dotted line.

5.2.2 Waalhaven

Table 5-1 shows the average sedimentation rate that is realized in the Waalhaven for different barrier heights. For a 3 m high barrier, for example, the sedimentation rate is reduced from 335 to 316 ton/day (minus 17 ton or - 5.80%).

Table 5-2 Sedimentation [ton/day] for different barrier heights in the entrance of Waalhaven.

Reference [ton/day]	1m barrier	2m barrier	3m barrier	4m barrier	5m barrier	6m barrier
335	333 (-0.74%)	**326** (-2.84%)	**316** (-5.80%)	**303** (-9.47%)	**289** (-13.78%)	**271** (-19.23%)

The results indicate that the sediment fluxes in and out of the Waalhaven are both diminished for larger barrier height. This is visualized in Appendix A.1. At the Waalhaven, the net effect is a reduction in sediment import. For a 3 m heigh barrier this amounts to -0.21 kg/s or 18 ton/day less sediment entering the basin. This is in the same order of magnitude as the reduction in sedimentation rate for a 3 m high barrier (Table 5-2: 316 – 333 = -17 ton/day).

Figure 5-2 shows how the reduction in sedimentation is spatially distributed over the basin. Again, the decrease in sedimentation is mostly observed in the direct proximity of the barrier and deeper in the basins (blue shades), and sedimentation increases in some parts of the basin (red shades). The concentrated increase in sedimentation near the basin's entrance may result in less dredging efforts in the the Waalhaven's side channels. More information

about the current dredging activities is required to quantify the potential savings in dredging costs and emissions.

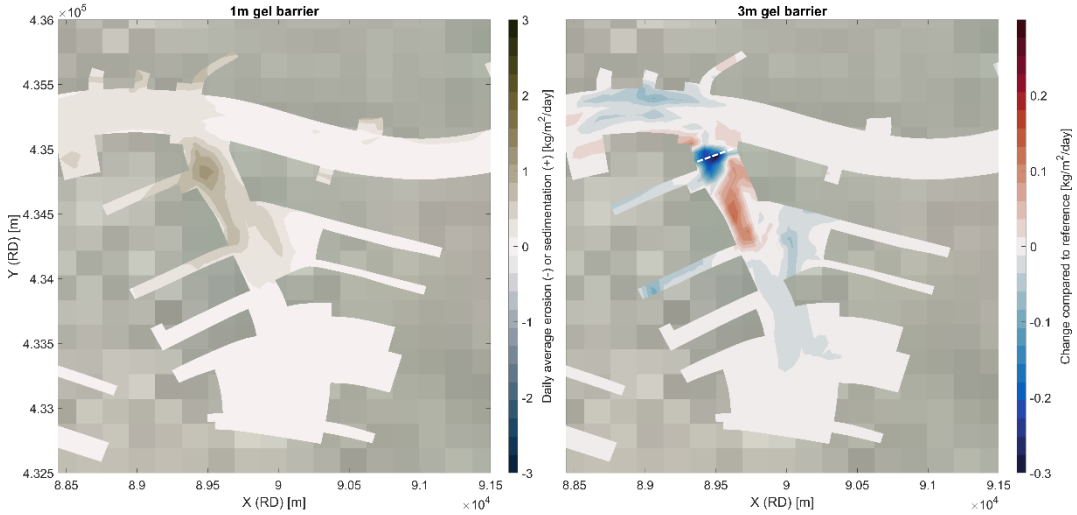

Figure 5-3 Change in spatial sedimentation patterns for a 3 m high barrier at Waalhaven. Left panel shows the daily average sedimentation rate in the simulation without a barrier. Right panel shows the relative increase/decrease in sedimentation rate for a 3 m high barrier. The approximate location of the barrier is indicated with the dotted line.

5.2.3 Calandkanaal

Table 5-3 shows the average sedimentation rate that is realized in the Calandkanaal for different barrier heights. For a 3 m high barrier, for example, the sedimentation rate stays roughly the same as in the situation without a barrier (+0.2%).

Table 5-3 Sedimentation [ton/day] for different barrier heights in the entrance of Waalhaven.

Reference [ton/day]	1m barrier	2m barrier	3m barrier	4m barrier	5m barrier	6m barrier
917	**916** (-0.05%)	**919** (+0.2%)	**927** (+1.1%)	**913** (-0.5%)	**879** (-4.2%)	**837** (-8.7%)

The results indicate that the sediment fluxes in and out of the Calandkanaal are less clearly affected for a larger barrier height compared to the other harbor basins. This is visualized in Appendix A.1. This might be partly explained by the large depth and relatively uniform sediment concentration profile (Appendix A.2). The high sediment concentrations higher up in the water column might make the barrier less effective in hampering sediment intrusion compared to the Botlek and Waalhaven (where most sediment is concentrated near the bottom). This hypothesis was elaborated in Section 5.1.

Figure 5-4 shows how the reduction in sedimentation is spatially distributed over the basin. Again, the decrease in sedimentation is mostly observed in the direct proximity of the barrier and deeper in the basins (blue shades). The sedimentation also increases in a large part of the basin (red shades). It seems unlikely that a barrier at this location would result in a decrease in dredging emissions, because the net sedimentation in the basin is hardly influenced for realistic barrier heights (< 4 m) and because there is an increase in sedimentation upstream in the river. In fact, the latter may in fact imply longer sailing distances to an offshore disposal site and thus higher dredging costs/emissions.

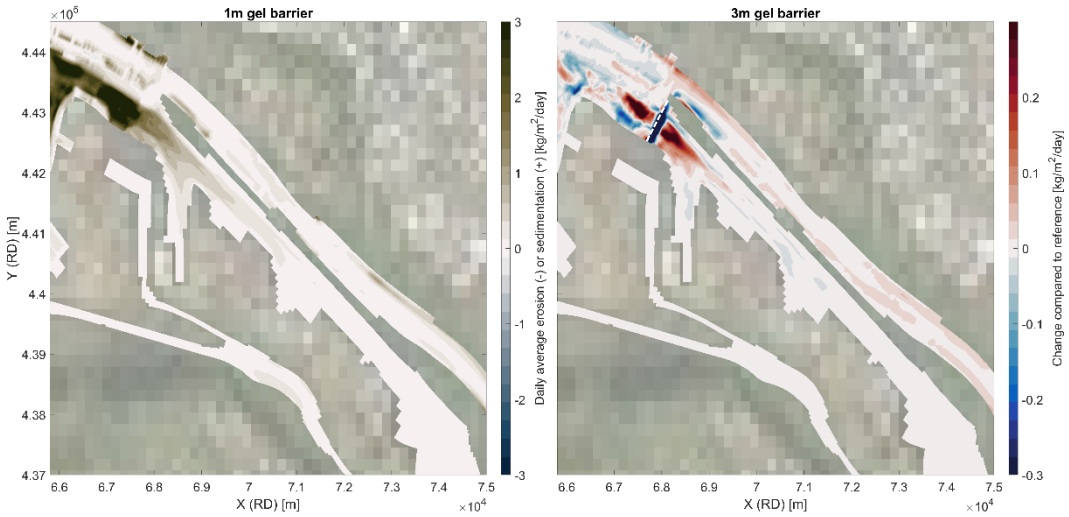

Figure 5-4 Change in spatial sedimentation patterns for a 3 m *high barrier at Waalhaven. Left panel shows the daily average sedimentation rate in the simulation without a barrier. Right panel shows the relative increase/decrease in sedimentation rate for a* 3 m *high barrier. The approximate location of the barrier is indicated with the dotted line.*

5.3 Where does the sediment go?

To study whether a decrease in sedimentation in one basin leads to an increase in sedimentation in another basin, we simulate a situation with only one singly barrier at Botlek/3PET. Table 5-4 shows the spatial redistribution of sedimentation in the Port of Rotterdam due to the placement of a 3 m high barrier at the entrance of Botlek/3PET.

Table 5-4 Spatial redistribution of sediment in the Port of Rotterdam due to the placement of a 3 m high barrier at entrance of Botlek + 3PET. These results are based on a simulation where only one barrier is implemented in the bathymetry of the Port of Rotterdam. The harbor areas are defined in Figure 2-5.

Harbor area	Reference (no barrier) sedimentation [ton/day]	Sedimentation for 3m barrier at Botlek only [ton/day]	Decrease (-) or Increase (+) in sedimentation [ton/day]
Botlek/3PET ***(behind barrier)***	1010.7	837.3	**-173 (-17.2%)**
Fruithavens	218.4	215.4	-3.00 (-1.37%)
Waalhaven	335.1	333.4	-1.68 (-0.50%)
Stadshaven	80.4	80	-0.36 (-0.44%)
Europoort (southern part only)	108.8	109.2	0.36 (+ 0.3%)
Calandkanaal (incl northern Europoort)	917.0	921.5	4.5 (+ 0.49%)
Pernis	396.1	400.7	4.53 (+ 1.14%)
Eemhaven	308.8	313.6	4.8 (+ 2%)
Rivers near Botlek < 15 km distance (including area directly in front of barrier)	1117	1254	**136 (+ 12.2%)**

The reduction in sedimentation in Botlek (-170 ton/day, see Table 5-4) is in the same order of magnitude as in the simulation where multiple barriers were implemented at once throughout the PoR (-170 ton/day, see Table 5-1). This gives confidence in the results in Table 5-1, which are based on simulations where multiple barriers are implemented at once under the assumption that there is little interaction between the different harbor basins on the time scale of a spring-neap cycle.

Table 5-4 shows that the decrease in sediment deposition in Botlek/3PET is two orders of magnitude larger than the increase or decrease in sediment deposition in neighboring basins. This suggests that the reduction in sediment deposition in Botlek/3PET is not compensated by an increase in sediment deposition in the neighboring basins.

The majority (80%) of the -173 ton/day that no longer settles in the Botlek/3PET basin is found to settle in the main waterways/rivers within a 15-km reach (136 ton/day, see Table 5 4). This is depicted in Figure 5-5.

The net effect of a barrier at the Botlek is favorable in terms of the sailing distance to an offshore disposal sight. The sailing distance is reduced for roughly 65% of the sediment mass that no longer settles in the Botlek: roughly 55% settles in front of the barrier (< 400m) and 10% settles even closer to the river mouth in the Scheur and Nieuwe Waterweg. For roughly 15% of the sediment mass which no longer settles in the Botlek, the sailing distance is increased. The remaining 20% either settles further away than 15 km from the basin or remains in suspension.

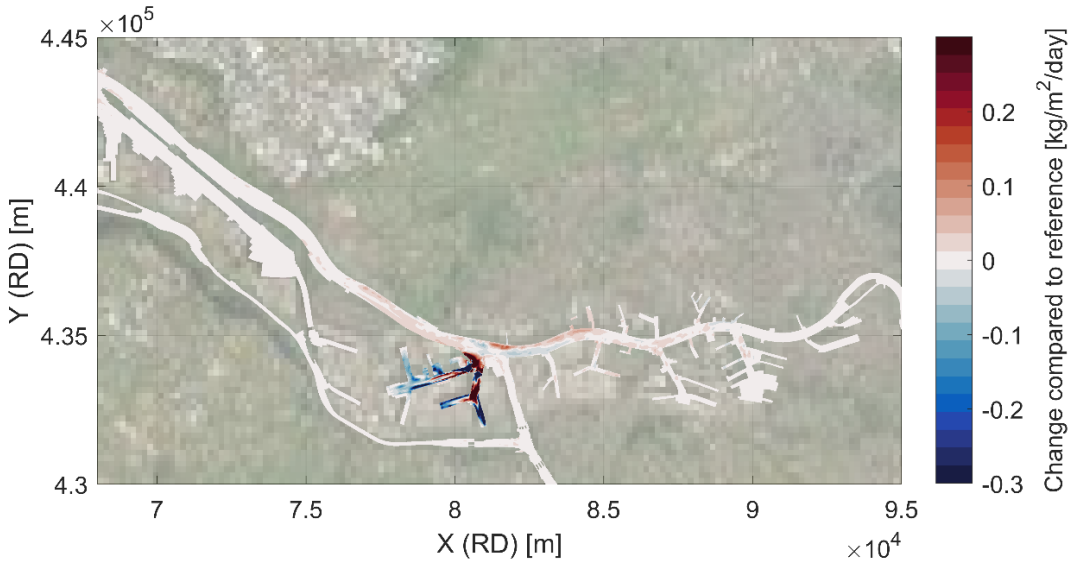

Figure 5-5 Spatial redistribution of sediment when a 3 m-heigh barrier is placed in the Botlek/3PET basin only. Results are based on the difference in sedimentation rate between the reference simulation (without a barrier) and the simulation with a barrier at the entrance of Botlek/3PET. Blue colors indicate the reduction in sedimentation in Botlek/3Pet. Red colors indicate where the sediment settles.

5.4 Discussion

The results suggest that the barrier is most effective in reducing sedimentation in the inland harbors, especially in the Botlek basin. Here, the sedimentation rate is reduced with roughly 17% for a 3 m-high barrier. In the deeper Calandkanaal, the barrier does not reduce sedimentation at all for realistic barrier heights (<4m).

5.4.1 How do gel barriers hamper sedimentation?

The results indicate that a higher barrier decreases both the influx and outflow of sediment in the harbor basins; the net effect of which can be a reduction in sedimentation.

A (larger) gel barrier is less effective in reducing sedimentation in basins where the layer with high sediment concentrations ($> 0.03\ kg/m^3$) reaches relatively high in the water column compared to the tip of the barrier (i.e. $H_{barrier}/H_{turbid}$ < 1). Here, the barrier seems less effective in reducing (suspended) sediment transport. The barrier seems most effective in the basins where most sediment is concentrated in the lower layer of the water column, such that $H_{barrier}/H_{turbid}$ > 1. This suggests that barriers are more effective in systems with little vertical mixing (e.g. stratified systems), whereas barriers are less effective in reducing sedimentation in systems with significant mixing and/or high sediment concentrations high in the water column. The optimal location and geometry for a gel barrier are not investigated in this study.

If vertical mixing of the water column is indeed an important process, this would be important to take into consideration when setting up a numerical model in a follow-up study. Although the current velocities round a small obstacle like a gel barrier are not validated in the present model, it is expected that the 20 vertical layers and $\kappa - \epsilon$ turbulence closure model give an adequate first impression of the barrier's effectiveness.

5.4.2 Does a gel barrier solve or merely shift the problem?

On the scale of a single basin, the decrease in sedimentation is mostly observed deeper in the basins. Interestingly, an increase in sedimentation is observed closer to the barrier. The shift of sedimentation towards the basin entrance may imply a decrease in sailing distance to an offshore disposal site, and therefore a reduction in dredging costs/emissions. Although we identify that a larger barrier height hampers the inflow and outflow of water (due to lower flow velocities), the present study does not research what hydrodynamic changes cause the change in sedimentation pattern.

On a system scale, the results suggest that the decrease in sedimentation in one basin, does not lead to an increase in sedimentation in the nearby harbor basins. Furthermore, the results suggest that roughly 65% settles closer to the river mouth, mostly in the river near the entrance of the Botlek (55%) and in the Scheur and Nieuwe Waterweg (10%). Only for about 15% of the sediment mass that no longer settles in Botlek, the sailing distance is expected to increase.

It must be stressed, however, that the 137 ton/day that is found to settle in the main waterways is a snapshot after one single spring-neap cycle. It is not studied on what time scale (and if) this sediment is resuspended and where it ends up at a longer time scale. In addition, 20% of the sediment was found to remain in suspension after two weeks (or to settle further away than 15 km from the Botlek). Understanding where the sediment ends up (spreading), and at what rate, would give insight in what additional dredging efforts would be required in the main waterways. This would require a longer simulation period, where time variation is taken into account (e.g. with multiple snapshots of the spatially varying sedimentation rate in time or with particle tracking). Nevertheless, it can be concluded that a gel barrier might reduce the required sailing distance for dredging activities by shifting the sedimentation location.

6 Conclusion & Recommendations

This research aimed to study the feasibility of a gel barriers to control sedimentation in the Port of Rotterdam (PoR). Based on lab experiments and numerical simulations, it can be concluded that the inland harbors of the PoR – such as Botlek – are most suitable to construct a barrier in terms of gel stability and the gel barrier's potential to reduce sedimentation. In inland harbors the flow conditions are generally mild, so that a gel barrier can withstand the natural flow currents and there is little vertical mixing which enhances its ability in steering sedimentation.

6.1.1 Conclusions

The lab experiments show the approximate gels' erosion thresholds which, in agreement with mud, are found to be two order of magnitudes smaller than the gels' Bingham Yield Stress (BYS). The 100 Pa BYS gel, which is expected to be navigable, remains stable (i.e. does not erode) for near-bottom velocities below 0.6 m/s. This gel is most suitable to construct a barrier in the more sheltered areas in the port like the entrances of Botlek/3e Petroleumhaven, Waalhaven and the Calandkanaal, where the tidal and river flow induced bed shear stresses remain below the gel's erosion threshold. For the parts of the port with stronger currents, the stiffer 400 Pa BYS gel might yield an outcome as its erosion threshold is expected to be > 1 m/s. However, it is uncertain if such a stiff gel is navigable on a pilot scale.

The CFD model is deemed useful to get a first indication on the exposure and damage realized by the propeller of a vessel, as it is found able to reproduce the experimentally determined erosion thresholds. The propeller jet of a representative large vessel that is expected to sail into Botlek several times per week is found to cause velocities near the gel barrier which are higher than the 100 Pa BYS gel's erosion threshold when the gap between keel and gel barrier is below 2 m. In those situations, damage to the gel barrier is expected to occur. It requires further research to investigate how effective a gel barrier is after a large vessel has passed with its keel close to the gel barrier and how a gel barrier could be maintained after such event.

The results of a large-scale sediment model transport suggest that the barrier is most effective in reducing sedimentation in the inland harbors with little vertical mixing and thus a concentrated near-bed layer of suspended sediment. While this research illustrates that a gel barrier is less effective in locations with more vertical mixing, it was not investigated what the optimal location and geometry would be for a gel barrier. Of the investigated locations, the barrier is found to be most effective in the Botlek/3Pet basin, where the sedimentation rate is reduced with roughly 17% for a 3 m high barrier. Most of this sediment mass (80%) settles within 15 km from the Botlek in the main waterways/rivers, 15% of which can be found landward leading to extra sailing distance for the dredger and 65% seaward leading to a reduction in sailing distance. Although this study does not quantify the potential saving in terms of costs or CO_2 emissions, these results suggest that a barrier could benefit dredging operations.

All in all, the gel barrier has a very attractive combination of features. It can limit and steer sedimentation and as material it has some strength while being flexible at the same time. The gel barrier has the potential to reduce dredging efforts (and, hence, costs and emissions), by reducing sailing distances and reducing dredging operations in less accessible and potentially contaminated basins. This applies especially to the inland harbors, such as the

Botlek. Gel barriers are especially effective in stratified systems and the effectiveness increases with a barrier height of more than 2m. The most important knowledge gaps are the costs of the gel barriers vs its benefits as well as the stability of the barrier in time under different failure mechanisms and the question of gel barrier effectiveness and required maintenance after ship propeller damage. Gel could also be applied for other applications as studied here, for example in a sediment trap to increase the sediment density, near dry docks, in an approach channel or near a quay wall which is a spot difficult to dredge, or to contain contaminated sediment within a confined area. However, before a field pilot may be carried out, there are still several open questions that need to be addressed first.

6.1.2 Recommendations

Phase 1 and phase 2 of this study serve as a feasibility study on the application of gel-barriers in a port. Some first important items have been studied and there is clearly a potential for beneficial applications. As this was the first study on this topic, there still is quite some room for further research before application in the harbor area can be considered.

It is recommended to continue with follow up research along different lines:

1. Evaluation of the added value of a gel barrier:
    - Investigate the costs of the gel barriers vs its benefits;
    - Economical placement/mixing strategies of gel in a port;
    - More detailed analysis of the influence of a gel barrier on dredging efforts and sailing distances;
    - Additional investigation of potential applications of a gel-barrier in a port.
2. Research on gel properties:
    - further optimization of the gel recipe e.g. via natural fiber reinforcements;
    - the time dependency of gel characteristics like strength, consistency and density;
    - the impact of gel degradation on nutrient loads and local water quality.
3. Research on gel barrier design:
    - different failure mechanisms like gel swelling and subsequent peeling off, gel-barrier tumbling or gel-barrier sliding;
    - the complex interactions between flow hydrodynamics, a gel barrier, and the sediment transported in the harbor;
    - the optimal location and shape of a barrier to reduce and steer sedimentation;
    - further investigation of navigability of gel barriers, in particular for > 100 Pa BYS gels;
    - larger-scale laboratory or flume tests with a gel-barrier;
4. Small-scale pilot field test to learn in practice.

It is logical and a relatively limited effort to start with line 1. When line 1 is finished lines 2 and 3 could be done simultaneously as there are interactions between them. When lines 1-3 are completed then it is recommended to start line 4 which is a small-scale pilot field test to learn in practice.

7 References

Argiolu, R. (2015). *MER Verdieping Nieuwe Waterweg, Botlek en 2e Petroleumhaven.* Arnhem: Arcadis.

Bampatzeliou, A., Daudey, P., Chassagne, C., Kirichek , A., de Wit, L., van Leeuwen, Y., . . . Renard, V. (2022). *Design of a Gel Product for sedimentation control in the Rotterdam port area.* Delft.

Cronin, K., de Wit, L., & Georgiou, M. (2021). *Sediment Trap Efficacy.* Delft: Deltares.

Cronin, K., Huismans, Y., & van Kessel, T. (2019). *Local mud dynamics and sedimentation around the Maasmond.* Delft: Deltares.

de Wit, L. (2015). *3D CFD modelling of overflow dredging plumes.* TU Delft.

Ding, J., Cheng, Y., Hua , Z., Yuan, C., & Wang, X. (2019). *The effect of dissolved organic matter (DOM) on the release and distrubtion of endocrine-disrupting Chemicals from sediment under hydrodynamic forces: A case study of Bisphenol A (BPA) and Nonylphenol (NP).* Environmental Science and Engineering.

Gust, G. (1989). *US Patent No. 4884892 A.*

Gust, G. (1990). *US Patent No. 4973165 A.*

Kirichek, A., Chassagne, C., Winterwerp, H., Noordijk, A., Rutgers, R., Schot, C., . . . Vellinga , T. (2018). How navigable are fluid mud layers? *PIANC-World Congress Panama City.* Panama.

Kirichek, A., Cronin, K., de Wit, L., Meshkati, E., van Keulen, D., & Terwindt, J. (2021). *Prisma I.* Delft: Deltares.

Man Diesel & Turbo. (2014). *Propulsion Trends in Bulk Carriers.* Copenhagen.

PIANC. (2015). *PIANC Report N. 180. Guidelines for protecting berthing structures from scour caused by ships.* Brussels : Martitime Navigation Commision.

Schiereck, G. J. (2019). *Introduction to Bed, bank and shore protection.* Delft: Delft Academic Press.

Soulsby , R. (1997). *Dynamics of marine sands: A manual for practical applications.* New York: HR Wallingford.

ten Brummelhuis, E. (2021). *Modelling of high concentration fluid mud water injection dredging density currents.* [Master's Thesis, Delft University of Technology].

van Kessel, T., van Rees, F., Talmon, A., & Mastbergen, D. (2021). *SO erosie sedimentatie slib.* Delft: Deltares.

van Kessel, T., Winterwerp, H., van Prooijen, B., van Ledden, M., & Borst, W. (2007). Modelling the seasonal dynamics of SPM with a simple algorithm for the buffering of fines in a sandy seabed. *INTERCOH'07*.

A Appendix

This appendix contains additional Delft3D results, which support the sedimentation analysis in Chapter 5.

A.1 Sediment fluxes over the gel barriers

The following figures show the influence of barrier height on sediment influx and outflow.

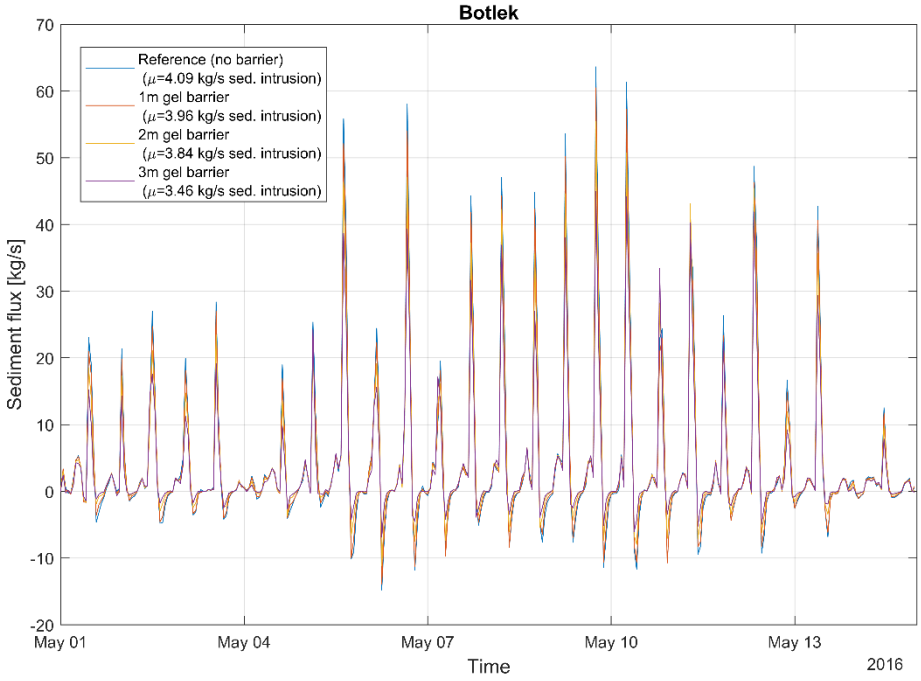

*Figure A-1 Sediment flux [kg/s] through the entrance of the **Botlek** harbor basin during a full spring-neap cycle. Positive values denote sediment being transported into the harbor, while negative values denote sediment leaving the harbor. Different colored lines represent simulations with different barrier heights. For each simulation the time-averaged flux (μ) is indicated in the legend.*

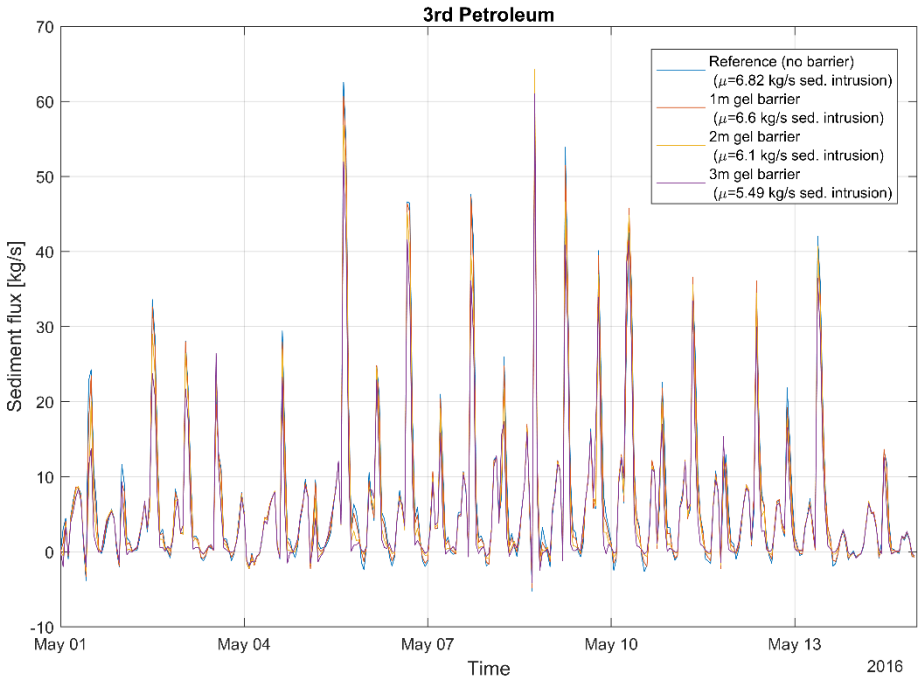

Figure A-2 Sediment flux [kg/s] through the entrance of the 3rd Petroleum harbor basin during a full spring-neap cycle. Positive values denote sediment being transported into the harbor, while negative values denote sediment leaving the harbor. Different colored lines represent simulations with different barrier heights. For each simulation the time-averaged flux (μ) is indicated in the legend.

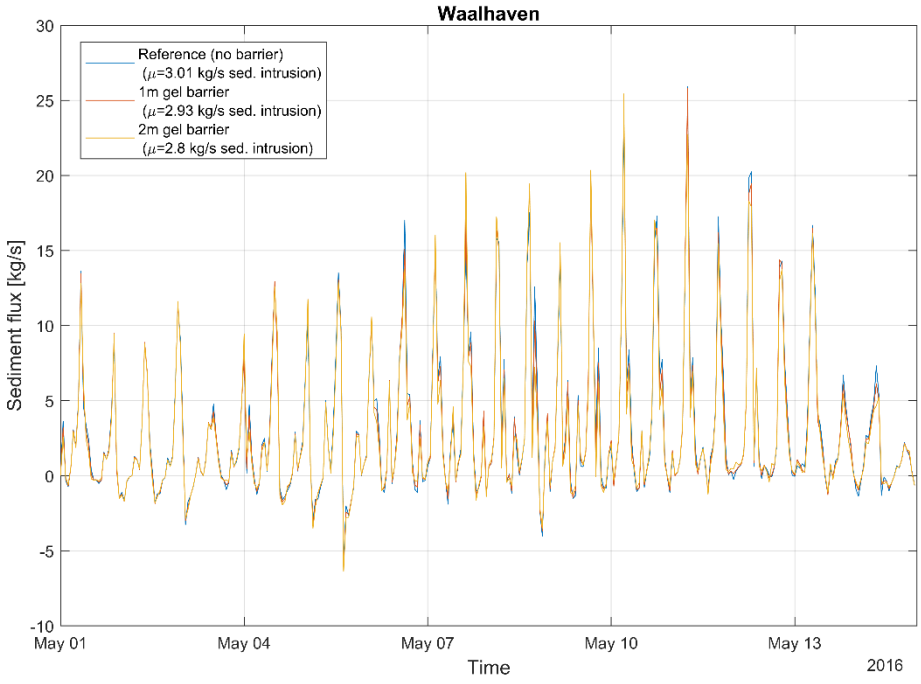

*Figure A-3 Sediment flux [kg/s] through the entrance of the **Waalhaven** basin during a full spring-neap cycle. Positive values denote sediment being transported into the harbor, while negative values denote sediment leaving the harbor. Different colored lines represent*

simulations with different barrier heights. For each simulation the time-averaged flux (μ) is indicated in the legend.

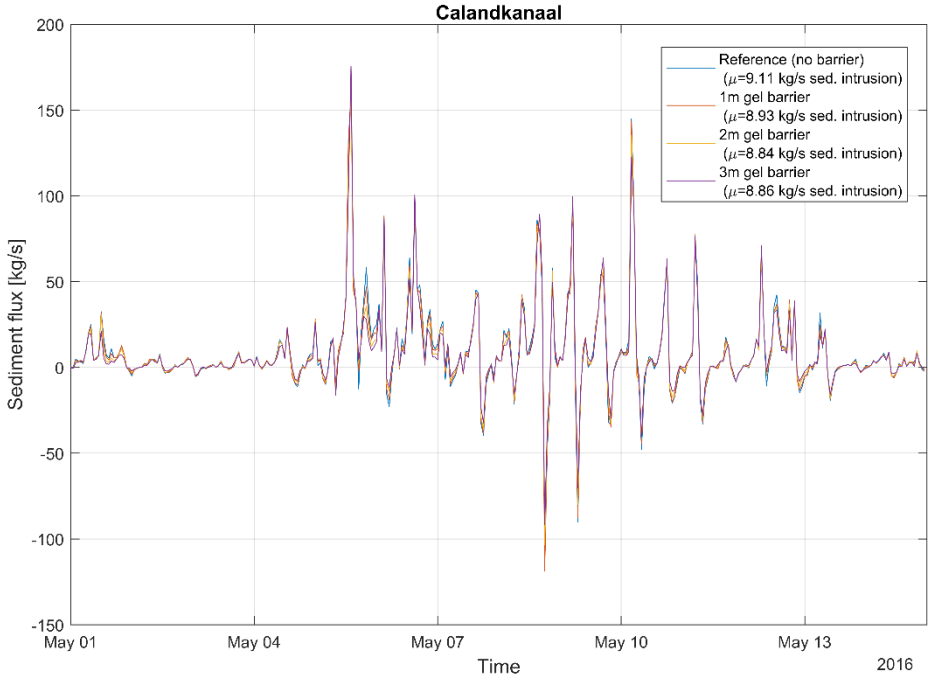

*Figure A-4 Sediment flux [kg/s] through the entrance of the **Calandkanaal** during a full spring-neap cycle. Positive values denote sediment being transported into the harbor, while negative values denote sediment leaving the harbor. Different colored lines represent simulations with different barrier heights. For each simulation the time-averaged flux (μ) is indicated in the legend.*

A.2 Vertical distribution suspended sediment

The following figures show the average suspended sediment concentrations in 2DV cross-section at both sides of the barriers at Botlek basin, Waalhaven and Beerkanaal. This is done to better understand the mechanisms for the reduction in sedimentation. For a higher barrier, the suspended sediment concentration at the harbor side of the barrier decreases, whereas it increases at the river side of the barrier.

Notice that in the Botlek basin (Figure A-5), the bottom layer of the water column with high sediment concentrations ($> 0.03\ kg/m^3$) is relatively thin compared to the barrier height. At Calandkanaal however, the barrier height remains relatively low compared to the thickness of this layer (Figure A-7).

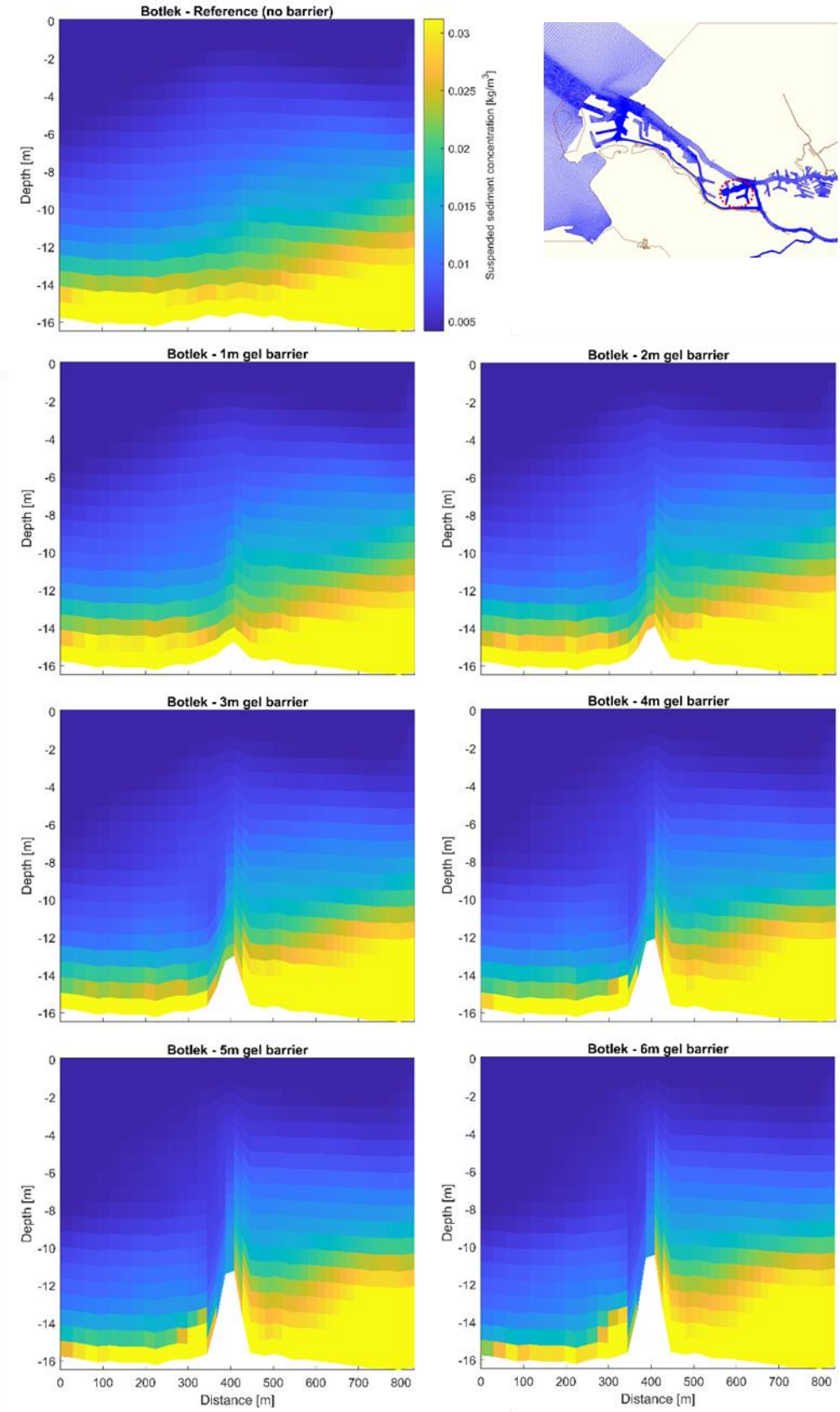

Figure A-5 Two-week spring-neap tide averaged SSC in a central vertical transect through the Botlek basin. The river is on the right-hand side of the barrier and the Botlek basin on the left-hand side.

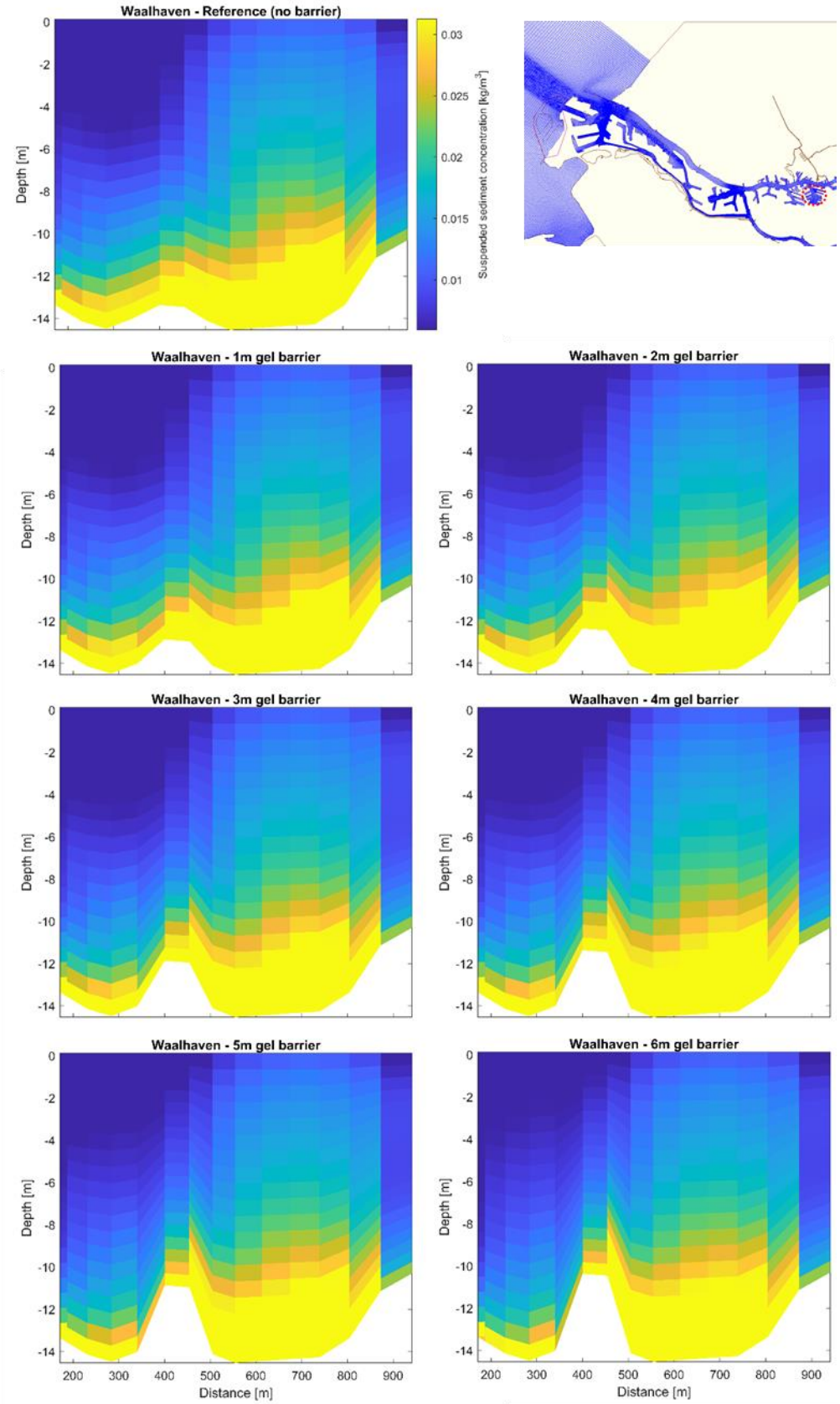

Figure A-6 Two-week spring-neap tide averaged SSC in a central vertical transect through the Waalhaven. The river is on the right-hand side of the barrier and the Waalhaven basin on the left-hand side.

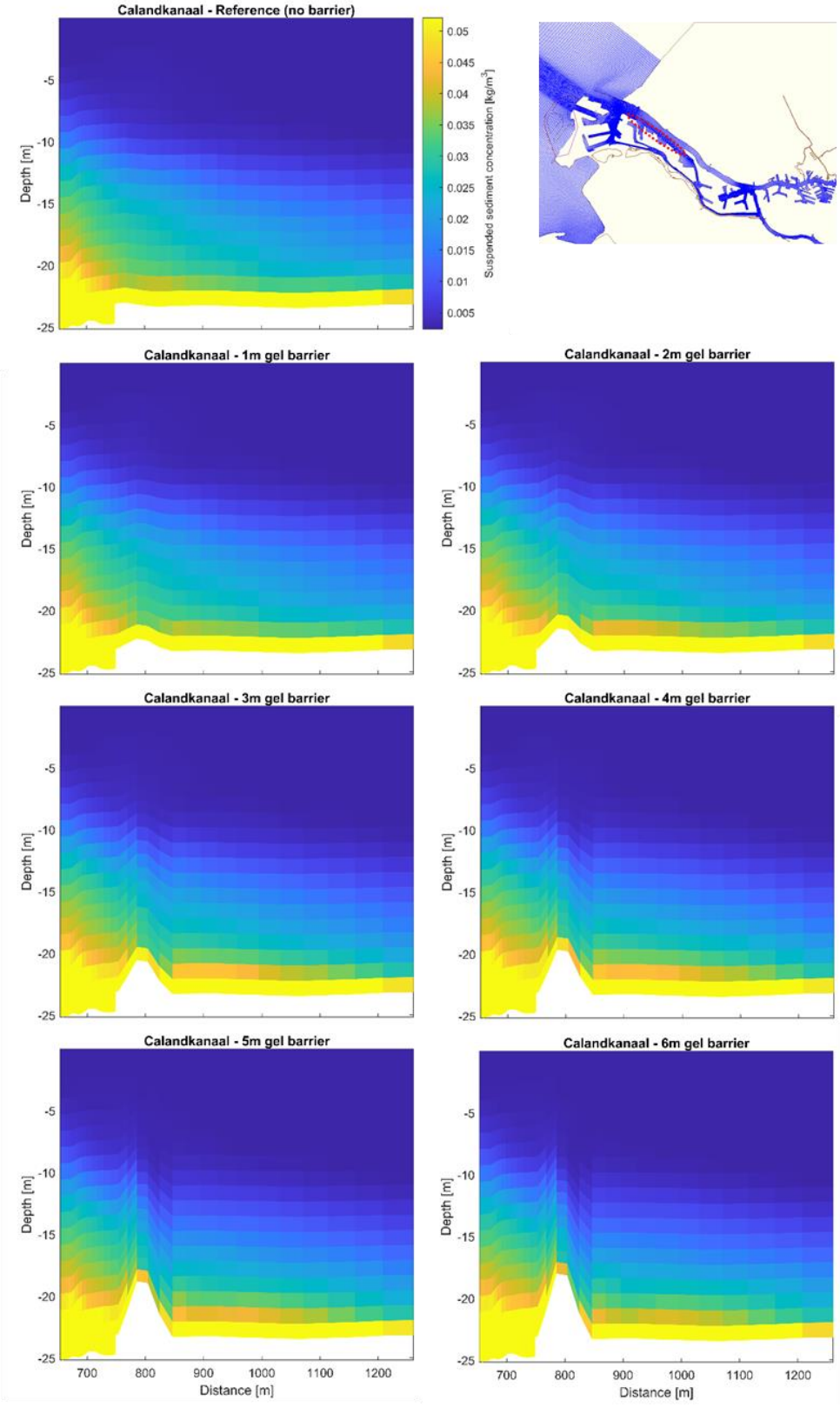

Figure A-7 Two-week spring-neap tide averaged SSC in a central vertical transect through the Beerkanaal. The mouth at the Beerkanaal is on the left-hand side of the barrier and the Calandkanaal is on the right-hand side.

Deltares is een onafhankelijk kennisinstituut voor toegepast onderzoek op het gebied van water en ondergrond. Wereldwijd werken we aan slimme oplossingen voor mens, milieu en maatschappij.

Deltares

www.deltares.nl